Article

Chinese Science Bulletin

Geology

October 2013 Vol.58 No.30: 3645–3663
doi: 10.1007/s11434-013-5842-y

Discovery of ~4.0 Ga detrital zircons in the Aermantai ophiolitic mélange, East Junggar, northwest China

HUANG Gang[1*], NIU GuangZhi[1], ZHANG ZhanWu[1], WANG XinLu[1], XU XueYi[2], GUO Jun[1] & YU Feng[1]

[1] *The Regional Institute of Shaanxi Bureau of Geological Exploration, Xianyang 712000, China;*
[2] *Xi'an Institute of Geology and Mineral Resource, Xi'an 710054, China*

Received November 16, 2012; accepted March 22, 2013; published online May 3, 2013

The East Junggar is an important part of the Central Asian Orogenic Belt (CAOB). Using *in situ* zircon dating and Hf isotopic analysis by LA-ICP-MS and MC-ICP-MS, respectively, a detrital zircon of ~4040 Ma age was found in sedimentary sequences from the Aermantai ophiolitic mélange, East Junggar. This is the oldest age record in the East Junggar terrane, and also marks the first zircon locality in the CAOB with an age older than 4.0 Ga, which is attributed to the Hadean crust. The ~4040 Ma detrital zircon has an $\varepsilon_{Hf}(t)$ value of –5.2 and a two-stage Hf modal age of 4474 Ma, suggesting the presence of very old (Hadean) crustal material in the source area. Beside peak ages of 446 Ma, we found four age groups of 3.6–3.1 Ga, 2.53–2.37 Ga, 1.14–0.89 Ga and 0.47–0.42 Ga from 141 effective measuring points. The age of 426±4 Ma for the five youngest detrital zircons defines the lower limit of the deposition time of sedimentary sequencess in the Aermantai ophiolitic mélange. The 0.47–0.42 Ga zircons exhibit $^{176}Hf/^{177}Hf$ ratios of 0.282156 to 0.282850, corresponding to variable $\varepsilon_{Hf}(t)$ values from –9.3 to 12.0 and Hf model ages from 2011 to 646 Ma. These characteristics are similar to those of the early Paleozoic igneous and gneissic zircons from the Altai, but significantly different from those of the East Junggar. Based on the material structures of felspathic greywacke, the morphology, internal texture and age distributions of dated detrital zircons, in combination with a study of the regional geological data, it is suggested that the sedimentary sequences in the Aermantai ophiolitic mélange was deposited in the Late Silurian, with the main provenance from the Altai Orogen in the north. This indicates that the early Paleozoic ocean represented by the Aermantai ophiolitic mélange was readily closed during the Late Silurian, and the northern edge of the East Junggar terrane was accreted to the Altai Orogen. The joint of them then served as a marginal orogen in the southern edge of the Siberia Paleocontinent.

East Junggar, Aermantai ophiolitic mélange, Hadean, detrital zircon, zircon U-Pb dating, Hf isotopes

Citation: Huang G, Niu G Z, Zhang Z W, et al. Discovery of ~4.0 Ga detrital zircons in the Aermantai ophiolitic mélange, East Junggar, northwest China. Chin Sci Bull, 2013, 58: 3645–3663, doi: 10.1007/s11434-013-5842-y

U-Pb dating and Hf isotope analysis of single detrital zircons from sedimentary rocks has been proven to be a powerful tool for tracing the source regions of sedimentary materials [1–5]. Zircons are able to withstand the effects of weathering, erosion, abrasion, and thermal alteration, and are difficult to destroy during transportation and deposition. Zircons are also abundant in intermediate–acid magmatic and high-grade metamorphic rocks, and thus record crustal magmatic and metamorphic events. As such, combined U-Pb dating and Hf isotope analysis of single zircon grains not only provides accurate ages, but can also provide insights into the possible source regions and provenance of sedimentary rocks, which can be linked to outcropping rocks and the tectonic evolution of the surrounding geological region [6–8]. In particular, zircon U-Pb age spectra for sedimentary samples provide geochronological constrains on the nature of ancient crustal terranes and also define the lower limit of the sediment deposition age [9–11]. Thus, detrital zircon U-Pb dating and Hf isotope analysis represents an unparalleled tool for the study of the nature and tectonic affinity of orogenic belts, as well as linking the erosion of such belts and the formation of sedimentary basin

*Corresponding author (email: hg1104220@yahoo.cn)

sequences [12,13].

Understanding the formation and early evolution of the Earth is an enduring challenge for researchers in the Earth Sciences. Some of the key scientific issues include the age of the earliest continental crust, the nature of this crust, and whether crust-mantle recycling occurred on the early Earth [14]. Rocks with Hadean ages (4.56–3.85 Ga) are rarely preserved today due to the intense modification of the Earth's surface by tectonism and erosion throughout Earth's history [15,16]. To date, crustal rocks with ages older than 3.8 Ga have only been found in Greenland [17,18], Canada [19,20], northeastern China [21–23], and eastern Antarctica [24–26]. The Acasta Gneiss from the Wopmay Orogen in Canada, with an age of ~4016 Ma, represents the oldest rocks that have been found on Earth [27]. Although very few rock suites that were produced during the earliest stages of the Earth have been discovered, abundant old zircons (⩾3.8 Ga) are present in younger geological units worldwide [28]. These include the northeastern Bavaria region of Germany [29], northern Wyoming in the USA [30], the Yilgarn craton of Western Australia [31], the San Francisco craton of Brazil [32], the high Himalayan region of western Nepal [33], and the Central Asian Orogenic Belt (CAOB) in northern Kazakhstan [34]. Detrital zircons with ages >4.0 Ga have been discovered in the Jack Hills region of the Yilgarn craton, western Australia, and the oldest zircon thus far dated has an age of ~4.4 Ga [31]. Recently, significant advances have been made in the search for extremely old rocks in China. Since the discovery of tonalite-trondhjemite-granodiorite (TTG) rocks with ages of 3.8 Ga in the Anshan area at the end of the last century, many areas have been shown to contain rocks with detrital zircons that yield ages >3.8 Ga, including Qianxi in Hebei Province [14,35–37], Pulan in the Tibet Autonomous Region [38,39], Yichang in Hubei Province [40], Liadang in Gansu Province [41,42], Pingle–Beijiang in southeast Guangdong Province [43], and Yushu in Qinghai Province [44]. Particularly notable amongst these studies was the discovery of zircons with ages of 4.1 Ga in the Pulan area of the Himalayan Orogen in China, and in the Liadang area of the northern Qinling Orogen. These ⩾3.8 Ga detrital zircons provide an excellent opportunity to further investigate the Earth's oldest crustal rocks and its early evolution.

Herein, we report a detrital zircon U-Pb age as old as ~4040 Ma from a sedimentary block within the Aermantai ophiolitic mélange, East Junggar, northwest China. This is the oldest zircon age from the East Junggar area, and also marks the first zircon locality in the CAOB to yield a Hadean age.

1 Geological background and samples

The Junggar terrane is situated in the central part of the CAOB and is traditionally divided into the Junggar Basin, East Junggar terrane, and West Junggar terrane (Figure 1(a)). The area studied in this paper is located in the central-northern part of the East Junggar terrane, and lies at the northeastern edge of the Junggar Basin. The East Junggar terrane is considered to be a Phanerozoic accretionary orogen, which is divided into the Altai Orogen to the north by the Irtysh fault zone and the Junggar Basin and Tianshan Orogen to the south by the Kalamaili fault zone [46,47]. Tectonically, the East Junggar terrane comprises, from north to south, the Dulate composite island arc, the Aermantai ophiolite mélange belt, the Yemaquan composite island arc, the Kalamaili ophiolite mélange belt, and the Jiangjunmiao accretionary complex. Due to its complex tectonic evolution, the East Junggar terrane and adjacent areas are a current focus of a range of geological studies [48–53].

The Aermantai ophiolitic mélange belt strikes SE-NW and is located in the central-northern part of the East Junggar terrane (Figure 1(b)). The belt extends from the northern slopes of the Beita Mountains near the China-Mongolia border, crosses the northern slopes of the Aermantai Mountains, and continues northwestwards along the Ulungur River to the Zhaheba area, where it is covered by Quaternary aeolian deposits of the Junggar Basin. The total length of the Aermantai ophiolite mélange belt is ca. 130 km. With the exception of sheeted dyke complexes, all the other rock types characteristic of ophiolite sequences are found in this ophiolitic mélange, including serpentinized harzburgites, dunites, pyroxenites, cumulate gabbros, dolerites, pillow basalts, massive basalts, and radiolarian-bearing siliceous rocks. These rock units crop out as tectonically bound slivers or blocks [55]. Banded chromites are occasionally found within the dunite rocks [56]. In addition, in the ophiolitic mélange in the Zhaheba area, Nb-enriched basalts and ultra-high pressure (UHP) rocks typically associated with an intra-oceanic arc have been discovered [57]. The UHP rocks are lherzolites with olivines that contain oriented masses of melted magnetite, garnet pyroxenites that contain high-Si and high-Ti garnets, quartz magnesites, and garnet amphibolites [58–60]. The presence of these rocks suggests that this region was once characterised by the ultra-deep subduction of oceanic crust. Throughout the extent of the belt, the ophiolite is tectonically emplaced above Late Palaeozoic volcano-sedimentary rocks. The northern boundary of the ophiolitic mélange transitions into a northwards-directed thrust belt. SHRIMP zircon U-Pb ages of gabbros and anorthosite granites from the Zhaheba ophiolite are 489±4 [61] and 496±6 Ma [62] respectively, and U-Pb ages of plagiogranites from the Aermantai ophiolite are 503±7 Ma [63], which appear to constrain the formation age of the ophiolite as being Late Cambrian to Early Ordovician.

This research is focused on sedimentary sequences within the Aermantai ophiolitic mélange. During the early 1990s, the Second Regional Geological Survey Team of the Xinjiang Bureau of Geology and Mineral Resources carried out a 1:50000 regional geological investigation in the Jieledekala

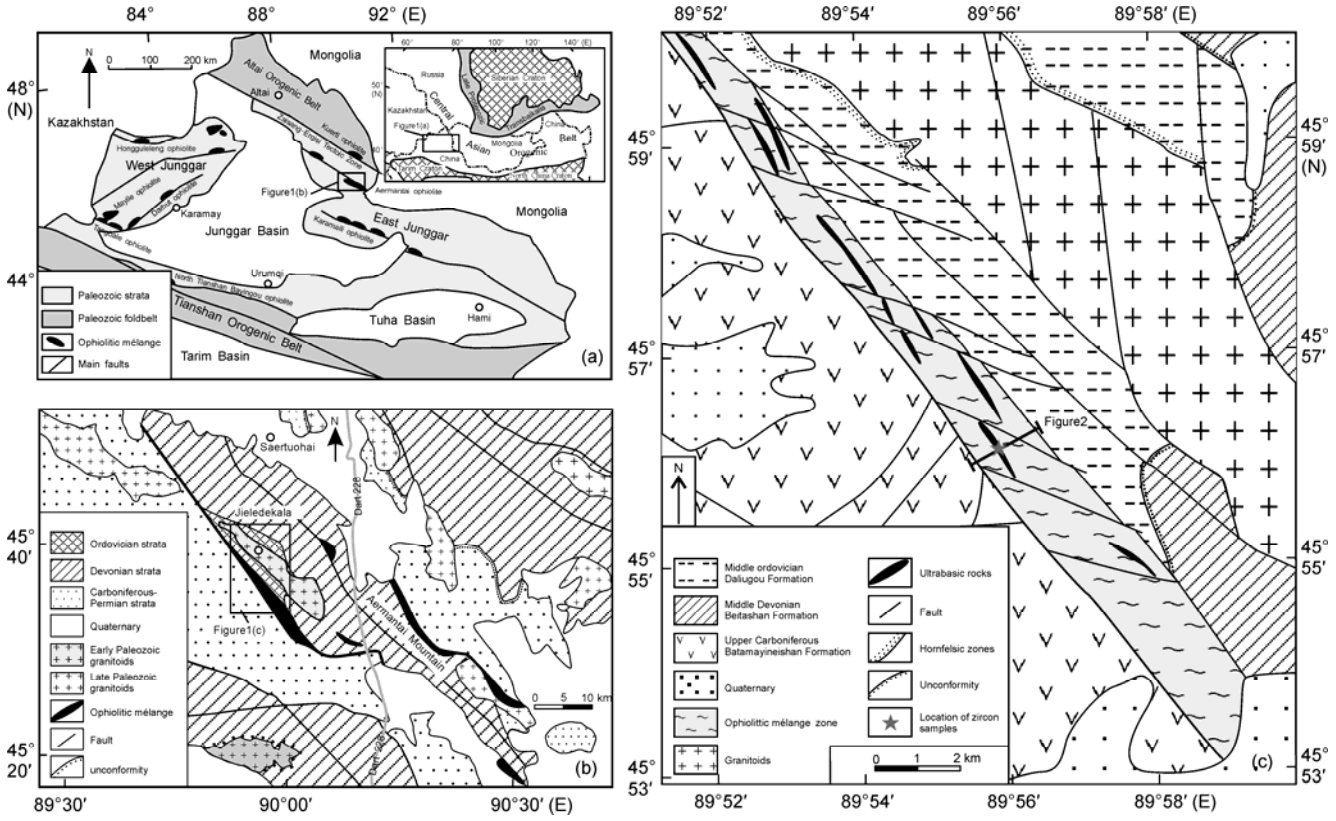

Figure 1 Simplified geological map of the Aermantai ophiolitic mélange and its adjacent areas. (a) Simplified geological map of the Junggar terrane (modified from Chen and Jahn [45]); (b) simplified geological map of the Aermantai area in the East Junggar (modified from Wang et al. [54]); (c) simplified geological map of the Jieledekala area in the East Junggar (modified from 1∶50000 ScaleJ ialepakeyizengde Regional Geological Survey Report [64]).

area. This investigation mapped the southern part of the Aermantai ophiolitic mélange, which was named the Jieledekala ophiolitic mélange (Figure 1(c)). This mélange is NW–SE trending, has an outcrop width of ca. 2 km, is separated from the Upper Ordovician Daliugou Formation on the north and the Upper Carboniferous Batamayineishan Formation on the south by faults, and is unconformably overlain by the Middle Devonian Beitashan Formation in the east [64]. Field observations have demonstrated that this ophiolitic mélange contains a range of rock types, including metamorphosed ultramafic rocks (serpentinite), gabbros, diorites, and siliceous rocks. These rock units crop out as lenses or irregular bodies, which are considered the tectonically dismembered sections of an ophiolite sequence. The ultramafic rocks have experienced intense metamorphism and alteration to become serpentinized dunites, serpentinites, and carbonate-rich rocks containing chromium spinel. The ophiolitic mélange also comprises volcanic and sedimentary sequences of various ages, including andesites, andesitic lava breccias, lithic sandstones, feldspathic rock fragment sandstones, and feldspathic greywackes (Figure 2), which represent forearc basin, back-arc basin, and/or continental slope deposits formed during the continent-ocean transition. Inclined and top-thick folds that are affected by ductile-brittle fracturing are widely developed throughout the ophiolitic mélange. The matrix of the mélange consists mainly of foliated fine-grained clastic and cataclastic rocks. A zircon U-Pb age of 508±4 Ma has been obtained from a meta-gabbro in the mélange. Considerable debate exists as to the age of the sedimentary sequences in the mélange, with published ages ranging from Middle Devonian [65–67] to Middle Ordovician [54,64]. Due to the lack of biostratigraphic and isotopic constraints, the age of the sedimentary blocks in the mélange is based on regional stratigraphy. The sample used in this study was obtained from a sandstone block in the mélange (45°56′04.2″N, 89°55′54.8″E), which is separated from the southern meta-ultramafic rocks (serpentinites) and the northern lithic sandstones by high-angle faults (Figure 2). The sample is a feldspathic greywacke, greenish to grey in colour, medium- to fine-grained, and layered in units of ca. 15 cm thickness. Petrographically, the rock consists of detrital material (60%–65%) and interstitial material (30%–35%). The detrital grains are mainly poorly sorted and angular quartz (30%–35%) and feldspar (25%–30%), with a typical grain size of ca. 0.15–0.30 mm. The interstitial materials are mainly sericite and chlorite, along with lesser amounts of calcite. The rock is matrix-supported and basal cemented, indicating that it has a low textural maturity and that the sediments were the product of a short transportation distance and rapid accumulation.

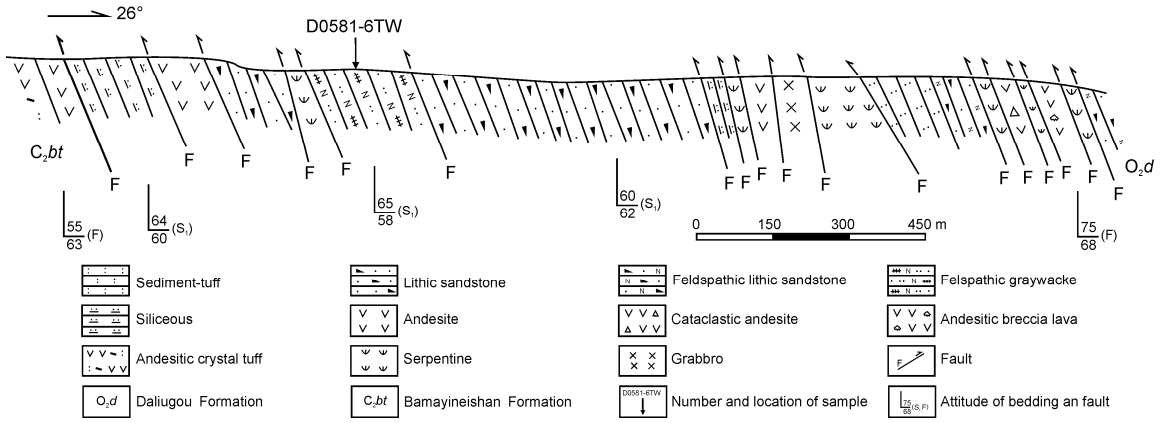

Figure 2 Geologic section of the Aermantai ophiolitic mélange.

2 Analytical methods

2.1 Sample preparation

Separation of zircon grains was conducted in the No. 203 Research Institute of Nuclear Industry, Xianyang, China, using conventional techniques, including heavy liquids, magnetic separation, and hand-picking under a binocular microscope equipped with ultraviolet light. Zircon grains were mounted in epoxy discs, polished to expose the zircon grains and then coated with gold. Prior to analytical work, polished surfaces were photographed in transmitted and reflected light to reveal the internal structure of the zircons. To further document the internal structure of the zircons and guide selection of sites for U-Pb dating and Hf isotope analyses, cathodoluminescence (CL) images were obtained with a CAMECA electron microprobe at the Institute of Geology and Geophysics, Chinese Academy of Sciences, Beijing, China. The acceleration voltage during CL imaging was 15 kV.

2.2 Zircon U-Pb dating

Zircon U-Pb dating was carried out with an Agilent 7500 a inductively coupled plasma-mass spectrometer (ICP-MS) coupled to a 193 nm laser at the Key Laboratory of Continental Collision and Plateau Uplift, Institute of Tibetan Plateau Research, Chinese Academy of Sciences (LCPU), Beijing, China and at the State Key Laboratory of Continental Dynamics (LCD), Northwest University, Xi'an, China. At LCPU, Plesovice [68] and Qinghu [69] natural zircons were used as matrix-matched, external standards for U-Pb dating and the NIST SRM612 glass was used as an external standard for trace element analysis. Analyses of Plesovice, Qinghu, and NIST SRM612 were made following every five sample analyses. At LCD, 91500 and GJ-1 natural zircons were used as external standards for U-Pb dating and the NIST SRM610 glass was used as an external standard for trace element analysis. Analyses of 91500, GJ-1, and NIST SRM610 were made following every six sample analyses. Isotope ratios and trace element concentrations were calculated off-line by GLITTER (Ver4.0, Macquarie University). Common Pb corrections and samples ages were calibrated and calculated using ComPb Corr#3.17[70]. U-Pb concordia diagrams, weighted mean age calculations, and U-Pb age probability density plots were made using Isoplot/Ex_ver 3 [71].

2.3 Zircon Lu–Hf isotope analysis

Hf isotope analyses of zircon were carried out at LCD using a Nu Plasma high-resolution, multiple-collector ICP–MS (Wrexham, UK) coupled to a Geolas 2005 laser ablation system equipped with a 193 nm ArF excimer laser. Zircons were ablated with a spot size of 32 μm, repetition rate of 10 Hz, and energy of 10 J/cm^2. The Hf isotope analytical procedures are similar to those described by Yuan et al. [72]. The isobaric interference of ^{176}Lu on ^{176}Hf was corrected by measuring interference-free ^{175}Lu and using a ^{176}Lu/^{175}Lu ratio of 0.02669 [73]. Similarly, the interference of ^{176}Yb on ^{176}Hf was corrected by measuring interference-free ^{172}Yb and using a ^{176}Yb/^{172}Yb ratio of 0.5886 [74]. Time-dependent drifts of Lu–Hf isotopic ratios were corrected using a linear interpolation method and interspersed analyses of 91500 zircon. ^{176}Hf/^{177}Hf ratios obtained for the zircon standards were 0.282295±27 (91500; n =17; 2σ) and 0.282049 ±23 (GJ-1; n = 10; 2σ). These standard results are in good agreement with the recommended ^{176}Hf/^{177}Hf ratios for these standards (0.2823075±58; 0.282015±19) [75,76]. The ^{176}Lu decay constant and chondritic ^{176}Hf/^{177}Hf and ^{176}Lu/^{177}Hf ratios used in our calculations are 1.865 × 10^{-11} y^{-1} [77], 0.282772, and 0.0332 [78], respectively. Single-stage model ages (T_{DM1}) were calculated relative to depleted mantle with present-day ^{176}Hf/^{177}Hf =0.28325 and ^{176}Lu/^{177}Hf =0.0384 [79]. Two-stage model ages (T_{DM2}) were calculated by assuming a mean ^{176}Lu/^{177}Hf value of 0.015 for average continental crust [80]. Initial ^{176}Hf/^{177}Hf ratios and $\varepsilon_{Hf}(t)$ values were calculated using zircon U-Pb ages.

3 Results

3.1 Zircon CL images

Zircons from the feldspathic greywacke sample D0581-6TW are pale pink or pink (ca. 5% are deep pink), transparent to translucent, and are mostly 70–170 μm in size. The internal structure and shape of the zircons allows them to be divided into two groups. The first group of zircons are mostly euhedral to subhedral and sub-angular (Figure 3(a)), which implies that these zircons have had a short transportation distance. Most zircons in this group exhibit zoning that is characteristic of magmatic crystallization. The second group of zircons are mostly subhedral to anhedral, but well rounded (Figure 3(b)–(d)), implying that these zircons have undergone long transportation distances. A small number of zircons in this second group have distinct cores and overgrown rims with variable widths, indicating metamorphism prior to transportation and deposition.

3.2 Zircon U-Pb ages

For zircon ages >1000 Ma, we adopted the $^{207}Pb/^{206}Pb$ age, and for ages <1000 Ma we adopted the $^{238}U/^{206}Pb$ age. We conducted 148 randomly selected analyses of zircons from sample D0581-6TW, which yielded 141 robust ages from 135 single zircon grains (Table 1). Analyses numbered 1–119 were carried out at LCPU and analyses 120–154 were carried out at LCD. The analyses enclosed by parentheses in Table 1 were not used in the statistical analysis of the data.

A small number of very old detrital zircon ages were obtained from the feldspathic greywacke sample, with the oldest being >4.0 Ga. Two analyses were conducted on this oldest zircon (analyses 32 and 138), yielding $^{207}Pb/^{206}Pb$ ages of 4043±5 and 4040±5 Ma, and Th/U ratios of 0.42 and 0.21, respectively. Both of these analyses are concordant at the 99% confidence level (Figure 4(a)), suggesting that these two ages are reliable. Petrographically, this zircon

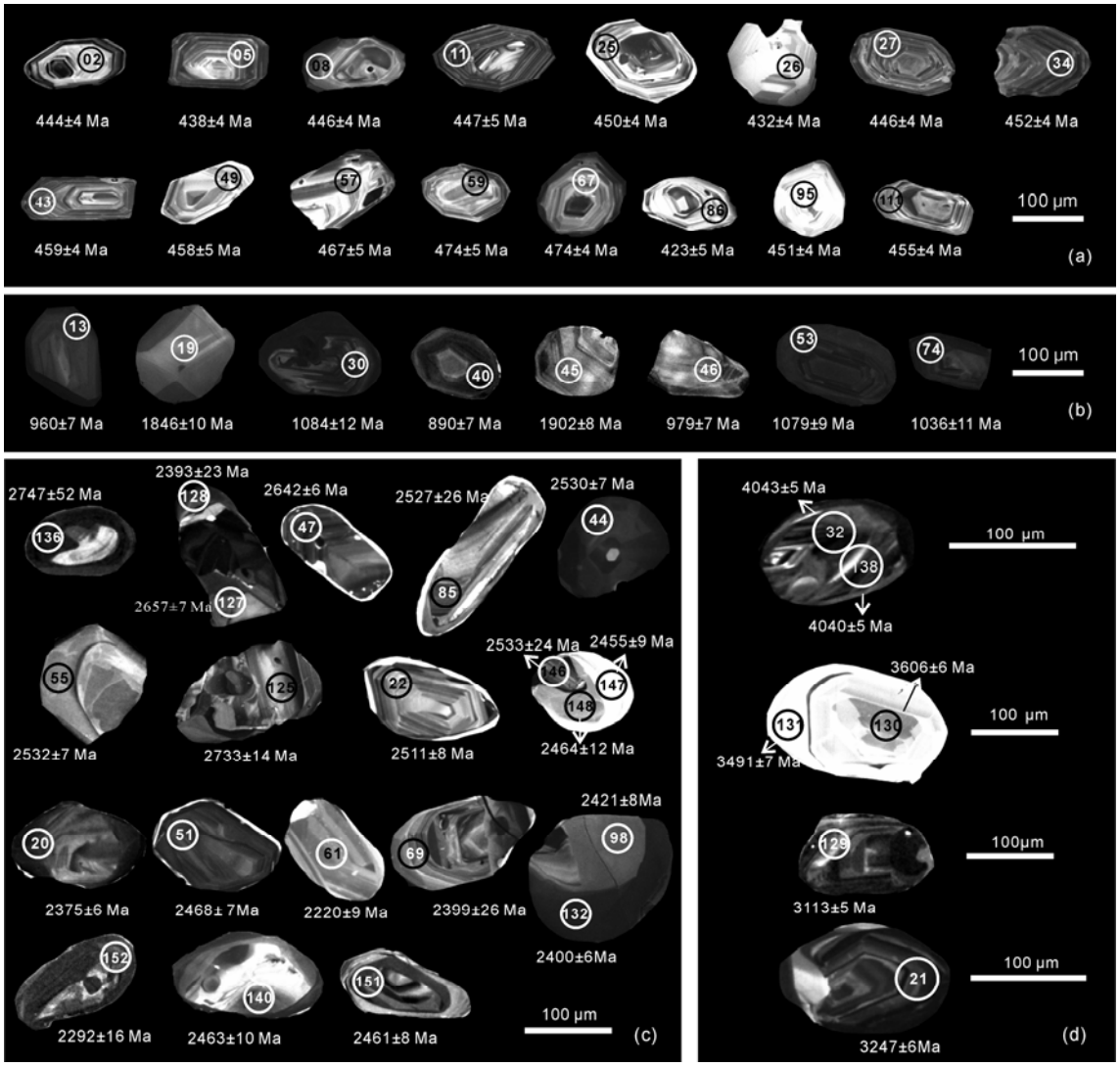

Figure 3 CL images of the detrital zircons with ages (a) <500 Ma, (b) 2000–800 Ma, (c) >3000 Ma and (d) 3000–2000 Ma.

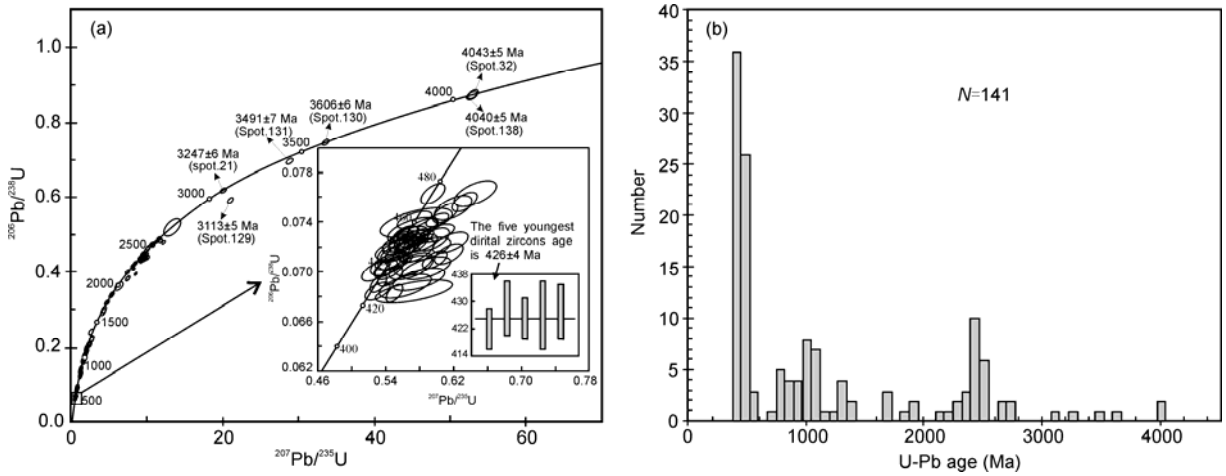

Figure 4 U-Pb concordia diagrams (a) and frequency chart (b) for detrital zircons from the sedimentary sequences in the Aermantai ophiolitic mélange.

grain is deep pink in colour, semi-transparent, and rounded. CL images show clear core-to-rim zoning in this zircon grain (Figure 3(d)). The inner core is ca. 10–15 μm in diameter and has a few wide and irregular growth bands. The surface of the mantle is slightly uneven, zoned, and has uniformly low CL. The narrow rim has no girdle and shows weak CL. These features and the high Th/U ratio suggest that this zircon is probably of magmatic origin. The two U-Pb analyses are from the mantle of the grain and, coupled with the age concordancy, indicates that the U-Pb isotope systematics of this zircon have remain closed to later tectonic processes.

Apart from these two U-Pb ages of >4.0 Ga, a number of other old and (nearly) concordant $^{207}Pb/^{206}Pb$ ages of 3606±6 to 3113±5 Ma were obtained (analyses 21, 129–131). Analyses 130 and 131 were obtained from the core and rim of the same zircon grain. CL images show that this zircon grain has well-developed core-to-rim zoning (Figure 3(d)), with a dark grey and unzoned inner core that has a high Th/U ratio (1.10). The mantle is weakly zoned and shows characteristics typical of a magmatic origin. The rim is white, has growth bands of variable width, exhibits no zoning, and has a low Th/U ratio (0.34). These features are typical of metamorphic zircon. The different $^{207}Pb/^{206}Pb$ ages of the core and rim probably represent at least two tectono-thermal events. $^{207}Pb/^{206}Pb$ ages of analyses 21 and 129 are 3247±6 and 3113±5 Ma, respectively, with Th/U ratios of 0.48. CL images show that these zircons have zoning typical of magmatic crystallization (Figure 3(d)).

A zircon U-Pb concordia diagram (Figure 4(a)) and age frequency plot (Figure 4(b)) show three main ages groups: 2.53–2.37, 1.14–0.89, and 0.47–0.42 Ga. The youngest group are the most abundant and includes 57 of the 141 robust U-Pb ages (ca. 40%). The peak age of this group is 446 Ma, and Th/U ratios vary between 0.46 and 1.33. The average age of the five youngest detrital zircons is 426±4 Ma. CL images show that the majority of these zircons are sub-angular and have obvious zoning (Figure 3(a)). All these characteristics are indicative of derivation from a nearby source area with a short transportation distance. The group with ages of 1.14–0.89 Ga has no obvious age peak, and represents a total of 23 ages (ca. 16%). Zircons in this age group are mostly sub-rounded, although a small number of grains are rounded. The cores of most of these zircons exhibit oscillatory zoning, and a small number of grains have obvious rims of variable width. Th/U ratios of these zircons vary from 0.02 to 1.76 (Figure 3(b)). The third group of zircons with ages of 2.53–2.37 Ga comprises 19 ages (ca. 14%). The age peak of this group is ca. 2.46 Ga and these zircons have Th/U ratios from 0.31 to 2.33. Most of the zircons in this group are sub-rounded and their internal textures allow them to be further divided into two types: one with thin metamorphic rims with clear zoning, and another with magmatic zoning and weak CL and relatively complex textures (Figure 3(c)).

3.3 Zircon Lu-Hf isotope data

Fifty-five Lu-Hf isotope analyses were conducted on 55 zircon grains from sample D0581-6TW (Table 2; Figure 5(a), (b)). All the zircons have low $^{176}Lu/^{177}Hf$ ratios (most are >0.002), indicating little accumulation of radiogenic Hf after zircon crystallization.

The zircons with ages between 0.47 and 0.42 Ga (n =24) have $^{176}Hf/^{177}Hf$ values from 0.282156 to 0.282850, $\varepsilon_{Hf}(t)$ values from –9.3 to +12.0, and two-stage model ages (T_{DM2}) of 2011–646 Ma. The zircons with ages of 1.14–0.89 Ga (n =12) have low $^{176}Hf/^{177}Hf$ values from 0.281721 to 0.282365, $\varepsilon_{Hf}(t)$ values from –16.8 to +7.8, and two-stage model ages (T_{DM2}) of 2868–1420 Ma. The zircons with ages of 2.53–2.37 Ga (n=8) have low $^{176}Hf/^{177}Hf$ values from 0.281104 to 0.281210, $\varepsilon_{Hf}(t)$ values from –7.0 to –0.5, and two-stage model ages (T_{DM2}) of 3513–3009 Ma, which are much older than the zircon U-Pb ages.

One analysis of the 4040 Ma zircon yielded a $^{176}Hf/^{177}Hf$ ratio of 0.280084 and $\varepsilon_{Hf}(t)$ value of –5.2. The single-stage

Table 1 Isotopic LA–ICPMS ages of detrital zircons from the sedimentary sequences in the Aermantai ophiolitic mélange, East Junggar

Spot	Th (ppm)	U (ppm)	Th/U	Isotopic ratios						Age (Ma)						Concordance (%)
				$^{207}Pb/^{206}Pb$	1σ	$^{207}Pb/^{235}U$	1σ	$^{206}Pb/^{238}U$	1σ	$^{207}Pb/^{206}Pb$	1σ	$^{207}Pb/^{235}U$	1σ	$^{206}Pb/^{238}U$	1σ	
01	124	256	0.48	0.06752	0.00158	1.32369	0.02879	0.14219	0.00121	854	50	856	13	857	7	100
02	169	278	0.61	0.05893	0.00204	0.57963	0.01933	0.07134	0.00067	564	77	464	12	444	4	105
03	587	669	0.88	0.05656	0.00179	0.55207	0.01680	0.07079	0.00061	474	72	446	11	441	4	101
04	263	253	1.04	0.06481	0.00220	1.10059	0.03580	0.12316	0.00116	768	73	754	17	749	7	101
05	172	211	0.82	0.05567	0.00120	0.53945	0.01086	0.07029	0.00062	439	29	438	7	438	4	100
06	193	365	0.53	0.06202	0.00126	0.63552	0.01198	0.07433	0.00065	675	25	500	7	462	4	108
07	193	135	1.42	0.07286	0.00137	1.59918	0.02786	0.15922	0.00143	1010	21	970	11	952	8	102
08	146	185	0.79	0.05831	0.00132	0.57604	0.01229	0.07166	0.00065	541	31	462	8	446	4	104
09	373	584	0.64	0.05914	0.00233	0.55983	0.02159	0.06867	0.00067	572	67	451	14	428	4	105
10	137	113	1.22	0.06183	0.00179	0.61648	0.01705	0.07233	0.00074	668	42	488	11	450	4	108
11	103	140	0.74	0.06097	0.00192	0.60343	0.01816	0.07179	0.00077	638	46	479	11	447	5	107
12	570	638	0.89	0.06031	0.00160	0.57448	0.01459	0.06910	0.00061	615	39	461	9	431	4	107
13	106	345	0.31	0.07336	0.00097	1.62335	0.01849	0.16052	0.00127	1024	11	979	7	960	7	102
14	333	269	1.24	0.05867	0.00120	0.58243	0.01104	0.07202	0.00063	555	26	466	7	448	4	104
15	525	647	0.81	0.05596	0.00087	0.53251	0.00736	0.06903	0.00055	451	17	433	5	430	3	101
16	183	171	1.07	0.05946	0.00160	0.59572	0.01522	0.07268	0.00071	584	38	475	10	452	4	105
17	231	806	0.29	0.06771	0.00102	1.19036	0.01542	0.12750	0.00099	860	32	796	7	774	6	103
18	285	290	0.98	0.06106	0.00132	0.59724	0.01207	0.07096	0.00064	641	28	475	8	442	4	107
19	104	155	0.67	0.11286	0.00146	5.30999	0.05932	0.34130	0.00285	1846	10	1870	10	1893	14	98
20	253	274	0.92	0.15258	0.00161	8.63814	0.07213	0.41069	0.00319	2375	6	2301	8	2218	15	107
21	127	265	0.48	0.25997	0.00264	21.26805	0.16871	0.59346	0.00464	3247	6	3151	8	3003	19	108
22	210	109	1.93	0.16534	0.00204	10.04548	0.10618	0.44073	0.00379	2511	8	2439	10	2354	17	107
23	217	359	0.60	0.06080	0.00108	0.59731	0.00971	0.07127	0.00060	632	21	476	6	444	4	107
24	84	407	0.21	0.07760	0.00109	1.98512	0.02329	0.18554	0.00144	1137	29	1110	8	1097	8	104
25	236	230	1.03	0.05795	0.00122	0.57705	0.01139	0.07224	0.00064	528	28	463	7	450	4	103
26	789	728	1.08	0.05957	0.00195	0.56943	0.01792	0.06933	0.00063	588	73	458	12	432	4	106
27	189	278	0.68	0.05572	0.00109	0.54991	0.00998	0.07160	0.00061	441	25	445	7	446	4	100
28 [a)]	180	202	0.89	0.09279	0.00199	0.93857	0.01859	0.07338	0.00071	1484	23	672	10	456	4	147
29	681	665	1.02	0.06005	0.00128	0.55016	0.01105	0.06646	0.00055	605	29	445	7	445	3	100
30	875	496	1.77	0.07558	0.00102	1.80127	0.02120	0.17289	0.00139	1084	12	1046	8	1028	8	105
31	91	112	0.81	0.05658	0.00253	0.57163	0.02485	0.07328	0.00078	475	102	459	16	456	5	101
32	154	362	0.42	0.43757	0.00425	53.02645	0.39295	0.87911	0.00672	4043	5	4051	7	4066	23	99
33	172	410	0.42	0.07525	0.00092	1.75629	0.01810	0.16932	0.00133	1075	10	1029	7	1008	7	107
34	336	503	0.67	0.05721	0.00156	0.57299	0.01481	0.07264	0.00063	500	61	460	10	452	4	102
35	458	461	0.99	0.06020	0.00198	0.58167	0.01862	0.07009	0.00064	611	53	466	12	437	4	107
36 [a)]	370	1050	0.35	0.17014	0.00175	7.22516	0.05788	0.30807	0.00237	2559	6	2140	7	1731	12	148
37	190	164	1.15	0.05910	0.00150	0.59657	0.01444	0.07323	0.00068	571	36	475	9	456	4	104
38	68	119	0.57	0.08927	0.00158	2.74830	0.04473	0.22333	0.00206	1410	17	1342	12	1299	11	109
39	381	645	0.59	0.07183	0.00084	1.59071	0.01535	0.16066	0.00124	981	9	967	6	960	7	101

(*To be continued on the next page*)

(*Continued*)

Spot	Th (ppm)	U (ppm)	Th/U	Isotopic ratios						Age (Ma)						Concordance (%)
				$^{207}Pb/^{206}Pb$	1σ	$^{207}Pb/^{235}U$	1σ	$^{206}Pb/^{238}U$	1σ	$^{207}Pb/^{206}Pb$	1σ	$^{207}Pb/^{235}U$	1σ	$^{206}Pb/^{238}U$	1σ	
40	39	517	0.08	0.07480	0.00091	1.52708	0.01568	0.14810	0.00116	1063	10	941	6	890	7	106
41	275	316	0.87	0.05866	0.00112	0.58168	0.01028	0.07193	0.00062	555	24	466	7	448	4	104
42	58	53	1.10	0.07114	0.00232	1.31062	0.04112	0.13365	0.00160	961	44	850	18	809	9	105
43	160	206	0.77	0.05872	0.00152	0.59736	0.01472	0.07381	0.00072	557	37	476	9	459	4	104
44	286	123	2.33	0.16722	0.00190	11.35925	0.10828	0.49281	0.00409	2530	7	2553	9	2583	18	98
45	85	167	0.51	0.11639	0.00140	5.42452	0.05514	0.33811	0.00276	1902	8	1889	9	1878	13	101
46	171	335	0.51	0.07254	0.00099	1.64028	0.01950	0.16406	0.00133	1001	12	986	7	979	7	101
47	128	258	0.50	0.17881	0.00186	12.07034	0.10031	0.48971	0.00386	2642	6	2610	8	2569	17	103
48	516	92	5.58	0.07326	0.00196	1.37140	0.03500	0.13581	0.00146	1021	34	877	15	821	8	107
49	214	173	1.24	0.06177	0.00201	0.62754	0.01956	0.07371	0.00081	666	48	495	12	458	5	108
50	84	95	0.89	0.05648	0.00350	0.57578	0.03487	0.07394	0.00097	471	141	462	22	460	6	100
51	133	294	0.45	0.16115	0.00172	9.63400	0.08314	0.43372	0.00345	2468	7	2400	8	2322	16	106
52	415	357	1.16	0.06016	0.00308	0.57505	0.02901	0.06935	0.00073	609	91	461	19	432	4	107
53	121	610	0.20	0.07539	0.00087	1.90456	0.01831	0.18329	0.00143	1079	9	1083	6	1085	8	100
54	425	529	0.80	0.06235	0.00149	0.61362	0.01383	0.07140	0.00068	686	32	486	9	445	4	109
55	80	142	0.57	0.16348	0.00182	10.97714	0.10131	0.48716	0.00399	2532	7	2521	9	2558	17	99
56	230	213	1.08	0.10225	0.00128	4.12274	0.04449	0.29254	0.00241	1665	9	1659	9	1654	12	101
57	65	120	0.54	0.05989	0.00187	0.61971	0.01853	0.07508	0.00081	600	46	490	12	467	5	105
58	73	82	0.89	0.06256	0.00258	0.70013	0.02789	0.08120	0.00107	693	62	539	17	503	6	107
59	117	103	1.14	0.06139	0.00205	0.64513	0.02072	0.07624	0.00086	653	49	505	13	474	5	107
60 [a)]	1202	1464	0.82	0.07853	0.00444	0.55377	0.03076	0.05114	0.00052	1160	115	447	20	322	3	139
61	95	115	0.83	0.13942	0.00175	7.73343	0.08442	0.40245	0.00347	2220	9	2200	10	2180	16	102
62	88	132	0.67	0.05891	0.00172	0.65429	0.01832	0.08058	0.00084	564	43	511	11	500	5	102
63	515	648	0.79	0.05905	0.00145	0.57422	0.01343	0.07055	0.00064	569	35	461	9	439	4	105
64 [a)]	564	665	0.85	0.08711	0.00125	2.02851	0.02577	0.16895	0.00142	1363	12	1125	9	1006	8	135
65	112	183	0.61	0.07182	0.00132	1.62838	0.02777	0.16451	0.00148	981	20	981	11	982	8	100
66	81	62	1.30	0.08376	0.00172	2.39213	0.04599	0.20720	0.00204	1287	22	1240	14	1214	11	106
67	275	262	1.05	0.05670	0.00119	0.59598	0.01170	0.07627	0.00068	480	28	475	7	474	4	100
68	60	128	0.47	0.07402	0.00131	1.75937	0.02854	0.17246	0.00154	1042	19	1031	11	1026	8	102
69	123	212	0.58	0.15476	0.00232	9.16584	0.11315	0.42956	0.00366	2399	26	2355	11	2304	16	104
70	654	976	0.67	0.07421	0.00139	1.52998	0.02684	0.14958	0.00124	1047	22	942	11	899	7	105
71	31	61	0.52	0.08864	0.00223	2.68105	0.06438	0.21945	0.00249	1396	29	1323	18	1279	13	109
72 [a)]	2998	1736	1.73	0.13253	0.00625	0.86441	0.03932	0.04730	0.00058	2132	85	633	21	298	4	212
73	209	225	0.93	0.10158	0.00123	4.23871	0.04380	0.30278	0.00247	1653	9	1682	8	1705	12	97
74	94	384	0.25	0.07381	0.00095	1.80244	0.02004	0.17718	0.00143	1036	11	1046	7	1052	8	98
75	141	194	0.73	0.08351	0.00120	2.78844	0.03581	0.24228	0.00206	1281	13	1352	10	1399	11	92
76	164	177	0.93	0.05768	0.00150	0.58364	0.01448	0.07342	0.00072	518	37	467	9	457	4	102
77	302	289	1.05	0.07674	0.00103	2.05747	0.02424	0.19455	0.00159	1114	12	1135	8	1146	9	97
78	208	169	1.23	0.05942	0.00269	0.77788	0.03432	0.09500	0.00118	583	74	584	20	585	7	100

(*To be continued on the next page*)

(*Continued*)

Spot	Th (ppm)	U (ppm)	Th/U	Isotopic ratios						Age (Ma)						Concordance (%)
				$^{207}Pb/^{206}Pb$	1σ	$^{207}Pb/^{235}U$	1σ	$^{206}Pb/^{238}U$	1σ	$^{207}Pb/^{206}Pb$	1σ	$^{207}Pb/^{235}U$	1σ	$^{206}Pb/^{238}U$	1σ	
79	483	406	1.19	0.06065	0.00116	0.63209	0.01119	0.07562	0.00066	627	23	497	7	470	4	106
80	109	155	0.71	0.10142	0.00155	4.07656	0.05647	0.29168	0.00263	1650	13	1650	11	1650	13	100
81	157	278	0.56	0.05923	0.00164	0.60745	0.01609	0.07442	0.00076	576	40	482	10	463	5	104
82	688	626	1.10	0.05898	0.00232	0.59314	0.02284	0.07297	0.00069	566	67	473	15	454	4	104
83	163	256	0.64	0.14683	0.00190	7.78867	0.08955	0.38491	0.00343	2309	9	2207	10	2099	16	110
84	144	224	0.64	0.05638	0.00184	0.55577	0.01733	0.07149	0.00067	467	74	449	11	445	4	101
85	92	205	0.45	0.16693	0.00254	10.06473	0.12432	0.43729	0.00390	2527	26	2441	11	2338	17	108
86	318	529	0.60	0.05832	0.00271	0.56649	0.02581	0.07048	0.00080	542	80	456	17	439	5	104
87 [a)]	638	674	0.95	0.07402	0.00389	0.69140	0.03553	0.06774	0.00076	1042	109	534	21	423	5	126
88	46	39	1.18	0.16410	0.00243	10.80015	0.14833	0.47751	0.00484	2498	11	2506	13	2516	21	99
89	82	161	0.51	0.05646	0.00188	0.56579	0.01826	0.07271	0.00074	471	53	455	12	452	4	101
90	193	172	1.13	0.05930	0.00265	0.58602	0.02554	0.07170	0.00086	578	74	468	16	446	5	105
91	290	244	1.19	0.16109	0.00165	10.79226	0.08927	0.48605	0.00386	2467	6	2505	8	2554	17	97
92	382	396	0.96	0.05898	0.00123	0.58271	0.01142	0.07167	0.00064	566	27	466	7	446	4	104
93	186	145	1.28	0.05843	0.00191	0.56577	0.01776	0.07025	0.00077	546	49	455	12	438	5	104
94	390	554	0.70	0.06297	0.00157	0.62658	0.01483	0.07218	0.00068	707	34	494	9	449	4	110
95	190	277	0.68	0.05777	0.00141	0.57723	0.01333	0.07249	0.00069	521	34	463	9	451	4	103
96	134	295	0.46	0.05564	0.00191	0.55034	0.01814	0.07174	0.00070	438	78	445	12	447	4	100
97 [a)]	981	1424	0.69	0.11499	0.00188	1.25764	0.01773	0.07932	0.00066	1880	30	827	8	492	4	168
98	120	132	0.91	0.15676	0.00187	9.86374	0.10196	0.45646	0.00394	2421	8	2422	10	2424	17	100
99	360	664	0.54	0.15811	0.00155	10.14146	0.07785	0.46529	0.00359	2436	6	2448	7	2463	16	99
100	182	141	1.29	0.05913	0.00182	0.57478	0.01696	0.07051	0.00075	572	46	461	11	439	5	105
101	395	485	0.81	0.05856	0.00098	0.55074	0.00840	0.06822	0.00057	551	19	445	6	425	3	105
102	98	255	0.38	0.05940	0.00224	0.74077	0.02731	0.09046	0.00088	582	63	563	16	558	5	101
103	92	125	0.74	0.06239	0.00284	0.60230	0.02660	0.07002	0.00096	688	71	479	17	436	6	110
104	256	218	1.18	0.05455	0.00116	0.52634	0.01048	0.06999	0.00062	394	29	429	7	436	4	98
105	227	242	0.94	0.07520	0.00181	1.34635	0.03064	0.12987	0.00133	1074	29	866	13	787	8	110
106	771	728	1.06	0.05951	0.00130	0.55505	0.01157	0.06765	0.00055	586	31	448	8	422	3	106
107	78	190	0.41	0.08523	0.00124	2.59285	0.03367	0.22067	0.00188	1321	13	1299	10	1285	10	103
108	232	210	1.11	0.05671	0.00128	0.54452	0.01162	0.06964	0.00064	480	31	441	8	434	4	102
109 [a)]	848	1684	0.50	0.10799	0.00252	1.64009	0.03529	0.11015	0.00100	1766	44	986	14	674	6	146
110	120	142	0.85	0.05606	0.00142	0.54262	0.01306	0.07021	0.00067	455	36	440	9	437	4	101
111	228	497	0.46	0.05956	0.00095	0.60026	0.00868	0.07310	0.00060	588	18	477	6	455	4	105
112	194	252	0.77	0.05990	0.00162	0.56621	0.01458	0.06856	0.00069	600	38	456	9	427	4	107
113	71	83	0.85	0.06692	0.00173	1.19030	0.02937	0.12900	0.00132	835	34	796	14	782	8	102
114	829	624	1.33	0.06005	0.00288	0.58326	0.02759	0.07044	0.00065	605	87	467	18	439	4	106
115	87	258	0.34	0.11654	0.00249	5.21950	0.09942	0.32483	0.00315	1904	39	1856	16	1813	15	105
116 [a)]	2334	1584	1.47	0.13018	0.00431	0.96749	0.03041	0.05390	0.00056	2100	60	687	16	338	3	203
117	160	260	0.61	0.06077	0.00409	0.57308	0.03816	0.06839	0.00082	631	124	460	25	426	5	108

(*To be continued on the next page*)

(*Continued*)

Spot	Th (ppm)	U (ppm)	Th/U	Isotopic ratios						Age (Ma)						Concordance (%)
				$^{207}Pb/^{206}Pb$	1σ	$^{207}Pb/^{235}U$	1σ	$^{206}Pb/^{238}U$	1σ	$^{207}Pb/^{206}Pb$	1σ	$^{207}Pb/^{235}U$	1σ	$^{206}Pb/^{238}U$	1σ	
118 [a]	1851	1840	1.01	0.26021	0.00264	11.79089	0.09429	0.32862	0.00259	3248	6	2588	7	1832	13	141
119 [a]	447	530	0.84	0.16276	0.00165	8.96043	0.07210	0.39926	0.00310	2485	6	2334	7	2166	14	115
120	122	188	0.65	0.05783	0.00167	0.66650	0.01800	0.08357	0.00074	523	44	519	11	517	4	100
121	205	449	0.46	0.07498	0.00095	1.82394	0.01724	0.17641	0.00108	1068	25	1054	6	1047	6	101
122 [a]	703	732	0.96	0.09431	0.00103	0.88513	0.00820	0.06807	0.00040	1514	21	644	4	425	2	152
123	67	132	0.51	0.05881	0.00142	0.64958	0.01439	0.08010	0.00063	560	34	508	9	497	4	98
124	42	114	0.37	0.07566	0.00128	1.89739	0.02758	0.18187	0.00129	1086	18	1080	10	1077	7	100
125	155	265	0.58	0.18898	0.00161	12.54532	0.07958	0.48146	0.00273	2733	14	2646	6	2534	12	104
126	200	375	0.53	0.05887	0.00123	0.60291	0.01135	0.07428	0.00054	835	45	479	7	462	4	96
127	105	181	0.58	0.18050	0.00215	12.67319	0.10942	0.50919	0.00343	2657	7	2656	8	2653	15	100
128	95	308	0.31	0.15416	0.00384	9.53248	0.22893	0.44843	0.00619	2393	23	2391	22	2388	28	100
129	224	462	0.48	0.23891	0.00257	20.42811	0.14196	0.62011	0.00386	3113	5	3112	7	3110	15	100
130	110	100	1.10	0.32758	0.00374	33.86259	0.27663	0.74966	0.00537	3606	6	3606	8	3606	20	100
131	12	37	0.34	0.30414	0.00374	29.19289	0.27609	0.69611	0.00548	3491	7	3460	9	3406	21	102
132	134	199	0.67	0.15485	0.00174	10.03890	0.07591	0.47016	0.00292	2400	6	2438	7	2484	13	98
133	22	897	0.02	0.07073	0.00098	1.45519	0.01597	0.14920	0.00094	950	13	912	7	896	5	98
134	104	461	0.23	0.07284	0.00122	1.70007	0.02435	0.16926	0.00114	1010	18	1009	9	1008	6	100
135	132	302	0.44	0.15976	0.00171	10.54255	0.07187	0.47857	0.00286	2453	5	2484	6	2521	12	99
136	49	822	0.06	0.19061	0.01077	13.67491	0.81706	0.52030	0.01932	2747	52	2727	57	2700	82	101
137	111	171	0.65	0.08234	0.00313	2.35788	0.08590	0.20768	0.00281	1254	50	1230	26	1216	15	101
138	59	284	0.21	0.43660	0.00477	53.35828	0.40365	0.88634	0.00621	4040	5	4057	8	4091	21	99
139	328	272	1.20	0.07334	0.00103	1.84776	0.02062	0.18273	0.00117	1023	13	1063	7	1082	6	98
140	115	168	0.69	0.16067	0.00225	10.34825	0.11731	0.46710	0.00359	2463	10	2466	10	2471	16	100
141	45	76	0.59	0.13419	0.00818	6.77089	0.40558	0.36595	0.01051	2154	65	2082	53	2010	50	104
142	138	174	0.80	0.05646	0.00133	0.62640	0.01356	0.08046	0.00062	471	34	494	8	499	4	101
143	184	355	0.52	0.06945	0.00097	1.58320	0.01763	0.16533	0.00105	912	13	964	7	986	6	98
144 [a]	154	624	0.25	0.09412	0.00110	1.68565	0.01408	0.12989	0.00105	1511	22	1003	5	787	6	127
145	20	160	0.12	0.06053	0.00141	0.71544	0.01524	0.08572	0.00067	623	32	548	9	530	4	97
146	148	217	0.68	0.16749	0.00239	10.37326	0.11000	0.44918	0.00428	2533	24	2469	10	2392	19	103
147	138	149	0.92	0.15992	0.00210	10.22350	0.10522	0.46366	0.00336	2455	9	2455	10	2456	15	100
148	57	65	0.88	0.16082	0.00251	10.31866	0.13777	0.46533	0.00399	2464	12	2464	12	2463	18	100
149	85	192	0.44	0.07273	0.00196	1.70493	0.04295	0.17002	0.00162	1006	36	1010	16	1012	9	100
150	72	484	0.15	0.07648	0.00110	1.96790	0.02277	0.18662	0.00122	1108	13	1105	8	1103	7	100
151	159	327	0.49	0.16049	0.00208	10.30074	0.10390	0.46548	0.00334	2461	8	2462	9	2464	15	100
152	77	846	0.09	0.14533	0.00266	8.59043	0.14190	0.42870	0.00415	2292	16	2296	15	2300	19	100
153	306	764	0.40	0.08474	0.00265	2.61642	0.07769	0.22393	0.00258	1310	40	1305	22	1303	14	100
154	121	206	0.59	0.07282	0.00138	1.71574	0.02887	0.17088	0.00128	1009	22	1014	11	1017	7	100

a) Discordia data. Concordance= (1−abs ($^{206}Pb/^{238}U$ age−$^{207}Pb/^{235}U$ age)/$^{206}Pb/^{238}U$ age) ×100%.

Table 2 Lu-Hf isotopes of detrital zircons of from the sedimentary sequences in the Aermantai ophiolitic mélange, East Junggar

Spot	Age (Ma)	$^{176}Yb/^{177}Hf$	$^{176}Lu/^{177}Hf$	$^{176}Hf/^{177}Hf$	2σ	$^{176}Hf/^{177}Hf_i$	$\varepsilon_{Hf}(0)$	$\varepsilon_{Hf}(t)$	T_{DM1} (Ma)	T_{DM2} (Ma)	$f_{Lu/Hf}$
01	463	0.016290	0.000644	0.282522	0.000010	0.282516	−8.8	1.2	1023	1366	−0.98
05	439	0.011286	0.000460	0.282239	0.000011	0.282235	−18.8	−9.3	1409	2011	−0.99
11	447	0.021350	0.000937	0.282320	0.000010	0.282312	−16.0	−6.4	1313	1834	−0.97
13	960	0.019839	0.000770	0.282304	0.000012	0.282290	−16.6	4.2	1330	1555	−0.98
14	448	0.051446	0.001988	0.282524	0.000012	0.282507	−8.8	0.5	1057	1396	−0.94
15	430	0.035498	0.001325	0.282535	0.000012	0.282524	−8.4	0.7	1023	1370	−0.96
16	452	0.010976	0.000412	0.282436	0.000010	0.282433	−11.9	−2.1	1136	1562	−0.99
18	442	0.014175	0.000697	0.282425	0.000014	0.282419	−12.3	−2.7	1159	1598	−0.98
19	1846	0.011751	0.000420	0.281642	0.000010	0.281627	−40.0	0.7	2221	2455	−0.99
20	2375	0.019902	0.000748	0.281104	0.000018	0.281070	−59.0	−7.0	2969	3331	−0.98
24	1137	0.025021	0.000967	0.282219	0.000012	0.282198	−19.6	4.9	1455	1646	−0.97
25	450	0.012537	0.000487	0.282444	0.000010	0.282440	−11.6	−1.8	1127	1546	−0.99
27	446	0.011233	0.000529	0.282543	0.000012	0.282539	−8.1	1.6	991	1328	−0.98
30	1084	0.060137	0.002272	0.282247	0.000018	0.282201	−18.6	3.8	1467	1675	−0.93
32	4043	0.018943	0.000758	0.280084	0.000012	0.280025	−95.1	−5.2	4326	4497	−0.98
33	1075	0.028497	0.001054	0.282003	0.000013	0.281982	−27.2	−4.2	1759	2167	−0.97
34	452	0.015606	0.000700	0.282398	0.000015	0.282392	−13.2	−3.5	1197	1652	−0.98
39	960	0.037159	0.001303	0.281721	0.000028	0.281697	−37.2	−16.8	2163	2868	−0.96
40	890	0.018719	0.000697	0.281941	0.000012	0.281929	−29.4	−10.1	1828	2401	−0.98
41	448	0.016600	0.000592	0.282697	0.000018	0.282692	−2.7	7.0	778	981	−0.98
43	459	0.015262	0.000630	0.282787	0.000010	0.282782	0.5	10.5	653	771	−0.98
44	2530	0.022147	0.000802	0.281093	0.000014	0.281054	−59.4	−4.0	2988	3266	−0.98
45	1902	0.034392	0.001280	0.281737	0.000012	0.281691	−36.6	4.2	2140	2279	−0.96
51	2468	0.009154	0.000402	0.281210	0.000010	0.281191	−55.2	−0.5	2801	3009	−0.99
52	432	0.027166	0.001061	0.282302	0.000014	0.282293	−16.6	−7.4	1343	1886	−0.97
53	1079	0.020877	0.000834	0.282300	0.000010	0.282283	−16.7	6.6	1338	1494	−0.97
55	2492	0.004332	0.000168	0.281106	0.000010	0.281098	−58.9	−3.3	2922	3195	−0.99
56	1665	0.024861	0.001125	0.281917	0.000012	0.281882	−30.2	5.6	1882	2011	−0.97
58	503	0.025402	0.001003	0.282280	0.000011	0.282271	−17.4	−6.7	1372	1891	−0.97

(*To be continued on the next page*)

(*Continued*)

Spot	Age (Ma)	$^{176}Yb/^{177}Hf$	$^{176}Lu/^{177}Hf$	$^{176}Hf/^{177}Hf$	2σ	$^{176}Hf/^{177}Hf_i$	$\varepsilon_{Hf}(0)$	$\varepsilon_{Hf}(t)$	T_{DM1} (Ma)	T_{DM2} (Ma)	$f_{Lu/Hf}$
59	474	0.013981	0.000574	0.282777	0.000010	0.282772	0.2	10.4	666	784	−0.98
66	2220	0.004843	0.000191	0.281105	0.000008	0.281097	−59.0	−9.6	2926	3372	−0.99
67	475	0.021502	0.000871	0.282450	0.000017	0.282442	−11.4	−1.2	1130	1525	−0.97
68	1042	0.016679	0.000642	0.282163	0.000012	0.282150	−21.5	1.1	1520	1814	−0.98
69	2399	0.012587	0.000490	0.281176	0.000010	0.281154	−56.4	−3.5	2853	3134	−0.99
74	1036	0.021580	0.000819	0.282292	0.000012	0.282276	−17.0	5.4	1348	1538	−0.98
76	457	0.013186	0.000566	0.282797	0.000012	0.282792	0.9	10.8	638	749	−0.98
77	1146	0.039358	0.001468	0.282305	0.000012	0.282273	−16.5	7.8	1353	1473	−0.96
78	585	0.029492	0.001086	0.282156	0.000012	0.282144	−21.8	−9.3	1548	2120	−0.97
79	470	0.015309	0.000640	0.282461	0.000010	0.282455	−11.0	−0.9	1108	1499	−0.98
83	2309	0.009402	0.000391	0.281181	0.000010	0.281164	−56.3	−5.2	2839	3170	−0.99
84	445	0.011363	0.000422	0.282278	0.000012	0.282274	−17.5	−7.8	1354	1920	−0.99
85	2527	0.018452	0.000702	0.281062	0.000012	0.281028	−60.5	−5.0	3022	3324	−0.98
92	446	0.020796	0.000834	0.282632	0.000014	0.282625	−5.0	4.6	874	1133	−0.97
92	446	0.012574	0.000531	0.282382	0.000010	0.282378	−13.8	−4.1	1214	1689	−0.98
95	451	0.011542	0.000528	0.282791	0.000009	0.282787	0.7	10.5	645	765	−0.98
98	2421	0.015720	0.000580	0.280999	0.000008	0.280972	−62.7	−9.4	3097	3513	−0.98
100	439	0.029437	0.001221	0.282444	0.000011	0.282434	−11.6	−2.3	1149	1567	−0.96
110	437	0.017607	0.000798	0.282516	0.000016	0.282509	−9.1	0.3	1035	1399	−0.98
112	427	0.014330	0.000498	0.282850	0.000009	0.282846	2.8	12.0	562	646	−0.99
133	950	0.016500	0.000667	0.282365	0.000010	0.282353	−14.4	6.2	1242	1420	−0.98
137	1254	0.023008	0.000823	0.281911	0.000010	0.281892	−30.4	−3.3	1875	2252	−0.98
142	499	0.024117	0.000957	0.282817	0.000014	0.282808	1.6	12.3	616	686	−0.97
143	986	0.016912	0.000617	0.282087	0.000010	0.282076	−24.2	−2.8	1624	2016	−0.98
152	2292	0.014986	0.000542	0.281201	0.000010	0.281177	−55.6	−5.1	2823	3151	−0.98
153	2453	0.016301	0.000627	0.281146	0.000012	0.281117	−57.5	−3.5	2903	3180	−0.98

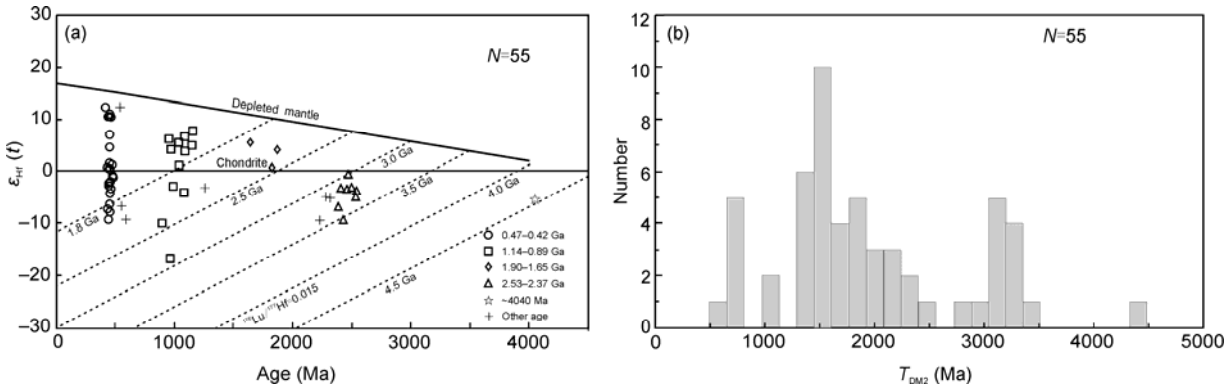

Figure 5 Hf isotopic feature (a) and Hf two-stage model ages histogram (b) of detrital zircons from the sedimentary sequences in the Aermantai ophiolitic mélange.

(T_{DM1}) and two-stage model ages (T_{DM2}) of this zircon are 4326 and 4474 Ma, respectively. The Lu/Hf ratio ($f_{Lu/Hf}$ = –0.92) of this zircon is much lower than the Lu/Hf ratio of continental crust ($f_{Lu/Hf}$ = –0.72; [81]), indicating that the two-stage model age (T_{DM2}) more accurately reflects the age when its source was extracted from the depleted mantle or the average crustal residence age of its source. As such, this old zircon is clearly of Hadean origin. The zircons with ages of 1.90–1.65 Ga (n = 3) have $^{176}Hf/^{177}Hf$ ratios of 0.281917 to 0.281642, $\varepsilon_{Hf}(t)$ values from 0.7 to 5.6, and two-stage model ages of 2455–2011 Ma, which indicates that their protolith originated from nascent continental crust.

4 Discussion

4.1 Discovery of 4.0 Ga detrital zircons

A total of 141 robust detrital zircon U-Pb ages were obtained from the feldspathic greywacke sample, and these range from 4.04 to 0.42 Ga. There are five detrital zircons whose U-Pb ages are >3.0 Ga, and one concordant zircon has a reliable age of 4.04 Ga. The other four old zircons have $^{207}Pb/^{206}Pb$ ages of 3606±6, 3491±7, 3247±6, and 3113±5 Ma. The 4.04 Ga detrital zircon age is the oldest obtained for crustal materials in the East Junggar terrane and the entire CAOB. Hf isotope analysis of this zircon shows that it has a $^{176}Hf/^{177}Hf$ ratio of 0.280084 and a $\varepsilon_{Hf}(t)$ value of –5.2. The single-stage (T_{DM1}) and two-stage model ages (T_{DM2}) of this ancient zircon are 4326 and 4474 Ma, respectively, which are similar to the 4.01–4.37 Ga zircons from the Jack Hills region of Australia [82]. Harrison et al. [82] suggested that Earth's continental crust began to form from ca. 4.4–4.5 Ga, but that this crust was recycled back into the mantle shortly after its formation. The Hf isotope compositions of the Jack Hills zircons are distinct from those of 3.8 Ga zircons in the North China and Yangtze cratons, which have Hf isotopes that are broadly chondritic and model ages of ca. 3.8 Ga, showing that they originated from a mantle source that had not experienced significant crust-mantle differentiation. As such, previous studies have suggested that crustal rocks older than 3.8 Ga do not exist in the north China area [14,83]. Given that the >3.0 Ga detrital zircons have probably experienced one or more transportation and recycling processes before their final incorporation in the sediment, their ultimate original source is difficult to determine. However, the identification of zircon grains with ages >3.0 Ga in this study and, in particular, the oldest zircon indicates that the East Junggar rocks record the recycling of old, Archaean and Hadean crustal materials. Kröner et al. [34] also dated one inherited zircon with a $^{207}Pb/^{206}Pb$ age of 3888±2 Ma from an Early Ordovician diorite porphyry in Stepnya, Kazakhstan, which is part of the western extension of the CAOB.

4.2 Constraints on depositional age and provenance

Sedimentary sequences of the Aermantai ophiolitic mélange have youngest detrital zircon U-Pb ages of 0.47 to 0.42 Ga. The main age peak is 446 Ma and the weighted average age of the five youngest detrital zircons is 426±4 Ma. This age represents the youngest erosional source and also is a lower limit for the sedimentary depositional age. As such, the sedimentary blocks in the Aermantai ophiolitic mélange must have been deposited no earlier than Middle Silurian times and, probably, even later (i.e. Devonian). The percentage of this group of young detrital zircons (Early Palaeozoic) is much higher than that of the old detrital zircons (pre-Early Palaeozoic). $\varepsilon_{Hf}(t)$ values of the young detrital zircons range from –9.3 to 12.0 and have two-stage model ages of 2011−646 Ma, which are much older than the formation age of the zircons. These young zircons are mostly euhedral or subhedral and angular, implying they have only experienced a short transportation distance. The two groups with older zircon ages of 1.14–0.89 and 2.53–2.37 Ga have $\varepsilon_{Hf}(t)$ values of –16.8 to 7.8 and –7.0 to –0.5, respectively, and two-stage model ages (T_{DM2}) of 2868–1420 and 3513–3009 Ma, respectively. The detrital zircons with ages of 2.53 to 2.37 Ga are characterised by negative $\varepsilon_{Hf}(t)$ values.

These features highlight the fact that the protolith of the old detrital zircons separated from the depleted mantle and entered the crust during the Archaean crustal accretion event. Most of the detrital zircons from these two older groups are rounded, indicating a relatively long transportation distance. This suggests that the sedimentary sequences in the Aermantai ophiolitic mélange were deposited in an area that experienced intense magmatism and was similar to modern sites of active continental marginal clastic sedimentation.

Recent studies have discovered evidence for Early Palaeozoic magmatism in the eastern Junggar terrane during a 1:25000 regional geological survey and other investigations. For example, we have obtained zircon U-Pb ages for quartz diorite and tonalite in the Yemaquan area that are 443±6 and 442±5 Ma, respectively (unpubl. data). Zhang et al. [84] reported a 442±7 Ma age for a deformed zircon core from a granitic porphyry in the Qiongheba area. In the Versailles area, Du et al. [85] obtained a moyite age of 429 Ma by U-Pb zircon dating. However, all these zircons have high $\varepsilon_{Hf}(t)$ values and relatively young two-stage model ages (>700 Ma) (Figure 6(a)), which precludes their use in constraining sandstone provenance. Many Early Palaeozoic intrusive rocks are also present in the Harlik Mountains, which is located at the southern edge of the East Junggar terrane. For example, near Harlik Koumenzi, diorite zircon has a U-Pb age of 430±6 Ma [86], and on the main ridge of the eastern Harlik diorite and granite, zircons have yielded U-Pb ages 447±11and 462±9 Ma, respectively [87]. These magmatic rocks are considered to be part of the active continental margin on the southern edge of the Turpan-Hami Basin, which has gradually migrated southwards during the Palaeozoic. The formation of these magmatic rocks is related to the northwards subduction of oceanic lithosphere, which is represented by relict oceanic crust in the Kangguertagg area [88]. Apparently, these tectonic blocks are not a potential provenance source for the sedimentary blocks in the Aermantai ophiolitic mélange. To the north of the studied area, at the southern edge of the Altay region,

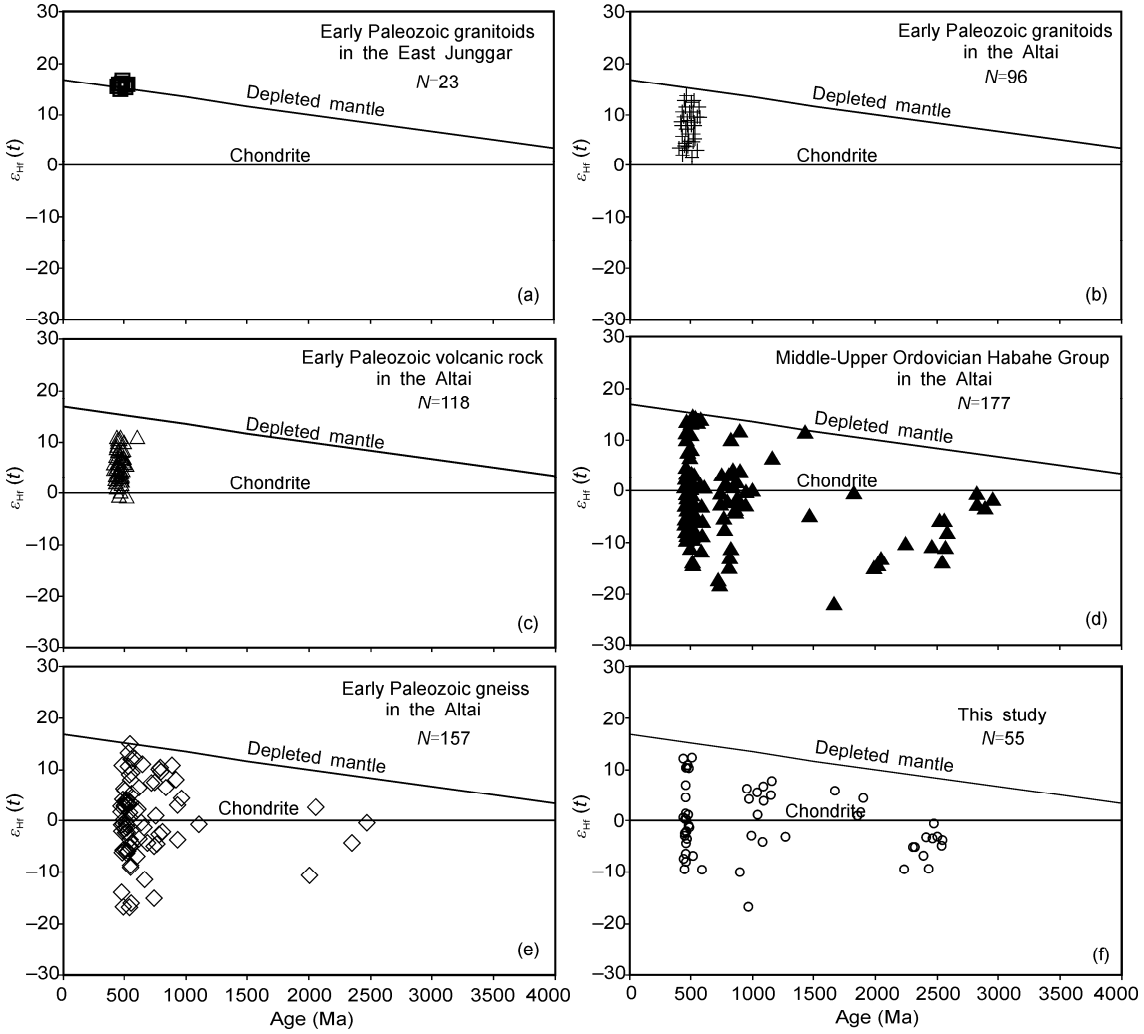

Figure 6 Comparison of probability plots of detrital zircon Hf isotope from the Paleozoic igneous rock and graywackes in the Chinese Altai and East Junggar. Data sources are as follows: (a) from Zhang et al. [84]; (b) from Sun et al. [52] and Cai et al. [97]; (c) from Wang et al. [98]; (d) from Long et al. [96]; (e) from Sun et al. [89]; (f) from this study (data with >3.6 Ga are excluded).

Early Palaeozoic granite, volcanic rocks, and gneiss are widely exposed [89–94]. For example, U-Pb ages of rocks in this region are as follows: Qiemurqieke gneissic granites: 462±10 Ma [90]; Seoul Basin volcanic rocks: 436±4 Ma [91]; Abagong gneissic syenogranite: 458±3 Ma [92]; Aergedayi meta-gabbro: 439±17 Ma [93]; Kelang Basin biotite granite: 459±5 Ma [94]. Recent studies have proposed that these Early Palaeozoic granites and volcanic rocks are subduction-related, syn-orogenic products that formed at an active continental margin [90–95]. Zircon $\varepsilon_{Hf}(t)$ values and two-stage model ages of these rocks are similar to those of Early Palaeozoic detrital zircons dated in our study (Figure 6(b) and (c)), thus suggesting that the Early Palaeozoic detrital zircons in our sandstone sample may largely originate from the northern Altai Orogen. In terms of Hf isotope composition and the distribution of detrital zircon ages (Figures 6(d), (e), 7(a), (b)), these sedimentary sequences are similar to gneisses of the Upper Ordovician Habahe Group in the Altai Orogen [96]. The sedimentary sequences also have a similar detrital zircon age distribution as the Ordovician Huangcaopo Group in the Yiwu of East Junggar (Figure 7(c)). These relationships indicate that all these units may share a similar provenance, with the provenance of the Ordovician Huangcaopo Group equivalent to the Altai Orogen in the north. This hypothesis is consistent with our results for the detrital zircons from the Aermantai ophiolitic mélange, but inconsistent with the Late Palaeozoic detrital zircon age spectrum of East Junggar (Figure 7(d)), which lies to the north of the Kalamaili ophiolitic mélange. Detrital zircons from East Junggar do not include Precambrian detrital zircon ages, and the provenance is probably from the volcano-sedimentary sequences deposited in the Palaeozoic island arc that once was south of East Junggar [53,99]. Early Palaeozoic and Precambrian detrital zircons have also been found in Carboniferous sandstones to the south of the Kalamaili ophiolitic mélange belt (Figure 7(e)), but its provenance is considered to be from southern areas that are now covered by the Tuha and Junggar basins [100]. In summary, detrital zircons reveal that the provenance of the sedimentary sequences in the Aermantai ophiolitic mélange is the Altai Orogen to the north. Given that the youngest detrital zircon age is 426±4 Ma, it is necessary to refine the depositional age of these sedimentary sequences as being Late Silurian rather than Devonian, as was previously considered to be the case.

4.3 Palaeozoic tectonic evolution of East Junggar and adjacent areas

The Aermantai ophiolitic mélange of East Junggar has detrital zircon U-Pb ages and Hf isotope signatures that indicate the sedimentary blocks may have been derived from the Altai Orogen in the Late Silurian. Recent studies have shown that the East Junggar terrane comprises a series of island arc mixtites and an accretionary wedge complex, which were produced by Palaeozoic subduction and accretion

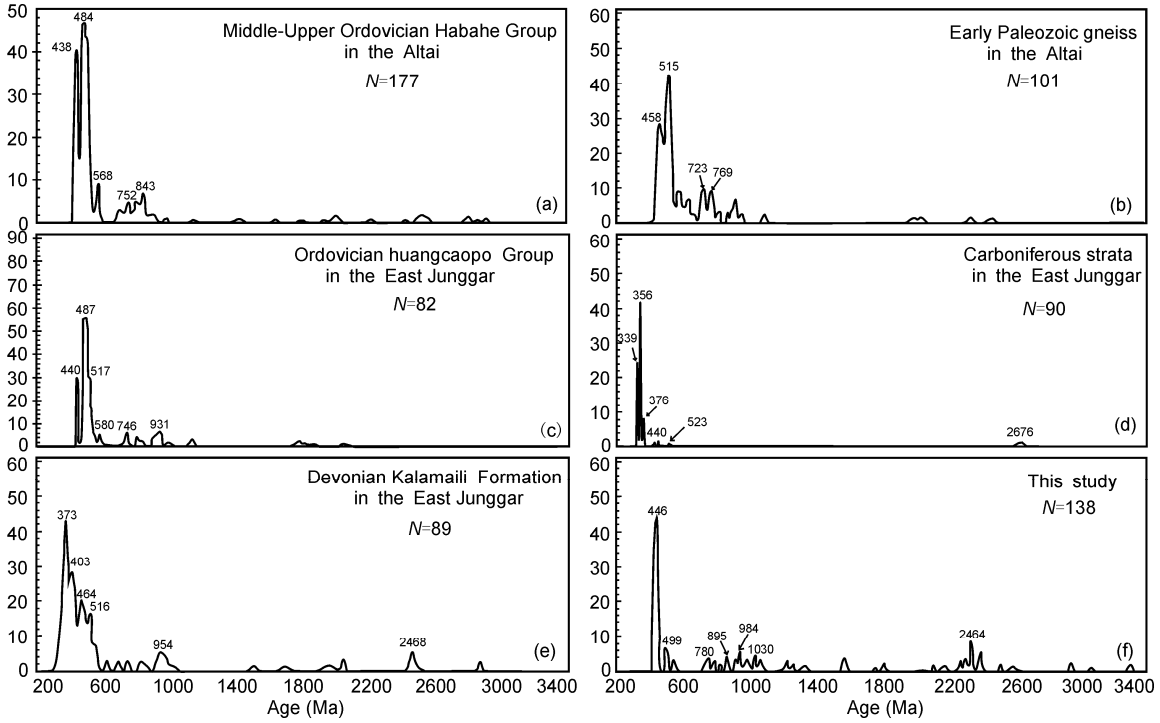

Figure 7 Comparison of probability plots of detrital zircon ages from the Paleozoic graywackes in the Chinese Altai and East Junggar. Data sources are as follows: (a) from Long et al. [53]; (b) from Sun et al. [52]; (c) from Long et al. [96]; (d) from Wang et al. [99]; (e) from Li et al. [100]; (f) from this study (data with >3.6 Ga are excluded).

[50,51]. From north to south, the East Junggar terrane is divided into the Dulate composite island arc, the Yemaquan composite island arc, and the Jiangjunmiao accretionary complex. These three tectonic units are separated by the Aermantai and Kalamaili ophiolite belts, which represent Early to Middle Palaeozoic oceanic crust [60,101]. However, the southern edge of the Altai Orogen lies to the north of the Aermantai and Irtysh tectonic belt, where an Early Palaeozoic active continental margin and an acidic magmatic arc were developed. These arc rocks have zircon ages between 470 and 440 Ma [90,95], which are slightly younger than the formation age (505–489 Ma) of the Aermantai supra-subduction zone type ophiolite [60–62]. In the northern part of the East Junggar terrane (Jieledekala area), zircon U-Pb ages of quartz diorite and granodiorite are 483±6 and 481±5 Ma respectively (unpublished data). The Jieledekala granodiorites are products of island arc magmatism, and represent the earliest magmatic event in the Early Palaeozoic. These granodiorites provide strong evidence for the subduction polarity of the oceanic lithosphere. From the Altai Mountains to the south of East Junggar, large-scale thrusts are characterised by oblique southwestwards movements that have overthrust younger rocks to the south [103,104]. Broadband seismic data for the East Junggar terrane reveal two strong, north-dipping reflectors at depths of 50 and 100 km between Kalamaili and Fuyun [104,105]. Moreover, from south Kalamaili to the Altai Mountains, the depth of the Moho gradually increases northwards, and there are bodies with anomalously high P-wave velocities below depths of 18–28 km that have a thickness of 10 km and a velocity of 7.3 km/s, similar to oceanic crust. At the northeastern edge of the Junggar Basin, deposition was continuous from the Middle Silurian to the base of the Lower Carboniferous. The main lithology of these sediments is terrestrial clastic rocks that are interbedded with minor carbonates, which have characteristics typical of passive continental margin deposits.

Based on the lines of evidence presented above, we suggest that the East Junggar Basin was characterised by gradual south-to-north subduction and, during subduction of the oceanic lithosphere, the subduction zone experienced a southward migration. During the Early Ordovician to Middle Silurian, an active marginal magmatic arc formed at the southern edge of the Altai Orogen due to northward subduction of Early Palaeozoic oceanic lithosphere as now represented by the Aermantai ophiolitic mélange. Middle to Late Silurian rocks of the East Junggar terrane are characterised by cold water biota such as *Tuvaella* fossils [106,107], which only occupied shallow waters at the southern edge of Siberia. Ordovician volcano-sedimentary sequences are unconformably overlain by Middle to Upper Silurian rocks with marine molasse features. These characteristics indicate that the Early Palaeozoic ocean basin system in the East Junggar area had closed by the Middle to Late Silurian and been accreted to the Siberia block to become the southern edge of the Siberia Paleocontinent. However, at this time, the region was still covered by a shallow sea that allowed *Tuvaella* to migrate across the southern edge of Siberia and reach East Junggar, including the area to the south of the Kalamaili ophiolite belt. Thus, we postulate that the Late Palaeozoic ocean basins located in the Irtysh and southern Mongolia, and the Late Palaeozoic ocean basins located in the southern Kalamaili must have existed within the interior of an enlarged Siberia Paleocontinent due to accretion of the East Junggar terrane. In effect, these ocean basins were underlain by continental crust. Late Silurian sedimentary sequences in the Aermantai ophiolitic mélange were mainly sourced from the Altai Orogen to the north, which shows that during the Late Silurian the northern edge of the East Junggar terrane was already part of the Altai Orogen. This became an integrated marginal orogen at the southern edge of the Siberia Paleocontinent and was the source of the sediments in the Aermantai ophiolitic mélange. Furthermore, the Early Palaeozoic ocean represented by the Aermantai ophiolitic mélange was closed by Late Silurian times.

5 Conclusions

(1) We have used LA-(MC)-ICP-MS zircon U-Pb dating to obtain a detrital zircon age spectrum for sedimentary sequences from the Aermantai ophiolitic mélange in East Junggar. The oldest determined zircon age is 4040 Ma. Hf isotope analysis of this zircon indicates that it has negative $\varepsilon_{Hf}(t)$ and a Hf isotope two-stage model age that is slightly older than its U-Pb age, demonstrating that even older continental crustal materials (Hadean) were present in its source. Other old detrital zircon ages of 3606±6 to 3113±5 Ma were also obtained. While it is difficult to infer the provenance of the >3.0 Ga zircons, their ages show that recycling of very old crustal materials with Mesoarchaean, Paleoarchaean, and Hadean ages are recorded by rocks of the East Junggar terrane.

(2) The youngest detrital zircon age is 426±4 Ma and defines the lower limit of the sediment depositional age. Considering the regional geology, the depositional age of sedimentary sequences in the Aermantai ophiolite mélange is probably Late Silurian.

(3) Detrital zircon U-Pb ages for the sedimentary sequences of the Aermantai ophiolitic mélange largely form three groups at 2.53–2.37, 1.14–0.89, and 0.47–0.42 Ga, with the main age peak being 446 Ma. The zircon ages, morphology, and internal structures, and Hf isotope data are consistent with the sedimentary provenance having been to the north in the Altai Orogen. During the Late Silurian, the Early Palaeozoic ocean represented by the Aermantai ophiolitic mélange closed and the northern edge of the East Junggar terrane had accreted to the Altai Orogen, which became an integrated marginal orogen on the southern edge of the Siberia Paleocontinent.

We thank Profs. Li Jingyi, Wang Yu, Yang Yongcheng and two anonymous reviewers for their constructive and valuable comments. We also thank Yuan Yahui, Wang Houqi, Li Shun and Zhang Jinyu for their help with zircon U-Pb dating and Hf isotope analyses.

1 Pell S D, Williams I S, Chivas A R. The use of protolith zircon age fringerprints in determining the protosource areas for some Australian the dune sands. Sedim Geol, 1997, 109: 233–360
2 Fedo C M, Sircombe K N, Rainbird R H. Detrital zircon analysis of the sedimentary record. In: Hanchar J M, Hoskin P W O, eds. Rev Mineral Geochem, 2003, 53: 277–303
3 Richards A, Argles T, Harris N, et al. Himalayan architecture constrained by isotopic tracers from clastic sediments. Earth Planet Sci Lett, 2005, 236: 773–796
4 Veevers J J, Saeed A, Belousova E A, et al. U-Pb ages and source composition by Hf-isotope and trace-element analysis of detrital zircons in Permian sandstone and modern sand from southwestern Australia and review of the palegeographical and denudational history of the Yilgarn Craton. Earth-Sci Rev, 2005, 68: 245–279
5 Veevers J J, Belousova E A, Saeed A, et al. Pan-Gondwanaland detrital zircons from Australia analysed for Hf-isotopes and trace elements reflect an ice-covered Antarctic provenance of 700–500 Ma age, T_{DM} of 2.0–1.0 Ga, and alkaline affinity. Earth-Sci Rev, 2006, 76: 135–174
6 Wan Y S, Li R W, Wilde S A, et al. UHP metamorphism and exhumation of Dabie Orogen: Evidence from SHRIMP dating of zircon and monazite from a UHP frantic gneiss cobble form the Heifei Basin, China. Geochimi Cosmochimi Acta, 2005, 69: 4333–4348
7 Wan Y S, Song T R, Liu D Y, et al. Mesozoic monazite in Neoproterozoic metasediments: Evidence for low-grade metamor-phism of Sinian sediments during Triassic continental collision, Liaodong Peninsula, NE China. Geochem J, 2007, 41: 47–55
8 Wan Y S, Liu D Y, Wang W, et al. Provenance of Mesoto Neoproterozoic cover sediments at the Ming Tombs, Beijing, North China Craton: An integrated study of U-Pb dating and Hf isotopic measurement of detrital zircons and whole-rock geochemistry. Gandwana Res, 2011, 20: 219–242
9 Bernet M, Spiedel C. Detrital thermochronology provenance analysis, exhumation, and landscape evolution of mountain belts. Geol Soc Am Spec Pap, 2004, 378: 1–126
10 Zhou J B, Wilde S A, Zhao G C, et al. SHRIMP U-Pb zircon dating of the Neoproterozoic Penglai Group and Archean gneisses from the Jiaobei Terrance, North China, and their tectonic implications. Precambrian Res, 2008, 160: 323–340
11 Lu S N, Li H C, Chen Z H, et al. Detrital zircon population of Proterozoic meta-sedimentary strata in the Qinling-Qilian-Kunlun Orogen (in Chinese). Acta Petrol Sin, 2009, 25: 2195–2208
12 Li R W, Wan Y S, Cheng Z Y, et al. Provenance of Jurassic sediments in the Heifei Basin, east-central China and the contribution of high-pressure and ultrahigh-pressure metamorphic rocks from the Dabie Shan. Earth Planet Sci Lett, 2005, 231: 279–294
13 Zhou J B, Wilde S A, Zhao G C, et al. SHRIMP U-Pb zircon dating of the Wulian Complex: Defining the boundary between the North and South China Cratons in the Sulu Orogenic Belt, China. Precambrian Res, 2008, 162: 559–576
14 Wu F Y, Yang J H, Liu X M, et al. Hf isotopes of the 3.8 Ga zircons in eastern Hebei Province, China: Implications for early crustal evolution of the North China Craton. Chin Sci Bull, 2005, 50: 1996–2003
15 Gradstein F M, Ogg J G, Smith A G, et al. A new geologic time scale, with special reference to Precambrian and Neogene. Episodes, 2004, 27: 83–100
16 Lu S N, Wang H C, Li H K. Unscramble the ISC 2004 and special reference to Precambrian from 2004 to 2008 (in Chinese). J Stratig, 2005, 25: 180–187
17 Kinny P D. 3820 Ma zircons from tonalitic Amitsoq gneiss in the Godthab district of southern West Greenland. Earth Planet Sci Lett, 1986, 79: 337–347
18 Nutman A P, Mojzsis S J, Friend C R L. Recognition of ≥3850 Ma water-lain sediments in West Greenland and their significance for the early Archaean Earth. Geochim Cosmochim Acta, 1997, 61: 2475–2484
19 Bowring S A, Housh T B, Isachsen C E. The Acasta gneisses: Remnant of Earth's early crust. In: Newsom H E, Jones J H, eds. Origin of the Earth. New York: Oxford Univ Press, 1990. 319–343
20 Iizuka T, Horie K, Komiya T, et al. 4.2 Ga zircon xenocryst in Acasta gneiss from northwestern Canada: Evidence for early continental crust. Geology, 2006, 34: 245–248
21 Liu D Y, Nutman A P, Compston W, et al. Remnants of 3800 Ma crust in the Chinese part of the Sino-Korean Craton. Geology, 1992, 20: 339–342
22 Song B, Nutman A P, Liu D Y, et al. 3800 to 2500 Ma crust in the Anshan area of Liaoning Provence, northeastern China. Precambrian Res, 1996, 78: 79–94
23 Wan Y S, Liu D Y, Song B, et al. Geochemical and Nd isotopic compositions of 3.8 Ga meta-quartz diorite and trondhjemitie rocks from the Anshan area and their geological significance. J Asian Earth Sci, 2005, 24: 563–575
24 Black L P, Williams I S, Compston W. Four zircon ages from one rock: The history of a 3930 Ma old granulite from Mount Sones, Enderby Land, Antarctica. Contrib Mineral Petrol, 1986, 94: 427–437
25 Harley S L, Black L P. A revised Archean chronology for the Napier Complex, Enderby Land, from SHRIMP ion-microprobe studies. Antar Sci, 1997, 9: 74–91
26 Choi S H, Mukasa S B, Andronikov A V, et al. Lu-Hf systematics of the ultra-high temperature Napier Metamorphic Complex in Antarctica: Evidence for the early Archean differentiation of Earth's mantle. Earth Planet Sci Lett, 2006, 246: 305–316
27 Sano Y, Terada K, Hidaka H, et al. Palaeoproterozoic thermal events recorded in the ~4.0 Ga Acasta gneiss, Canada: Evidence from SHRIMP U-Pb dating of apatite and zircon. Geochim Cosmochim Acta, 1999, 63: 899–905
28 Wan Y S, Liu D Y, Dong C Y, et al. The oldest rocks and zircons in China (in Chinese). Acta Petrol Sin, 2009, 25: 1973–1807
29 Gebauer D, Williams I S, Compston W, et al. The development of the Central European Continental crust since the Early Archaean based on conventional and ion-microprobe dating of up to 3.84 Ga old detrital zircons. Tectonophysics, 1989, 157: 81–96
30 Mueller P A, Wooden J L, Nutman A P, et al. Early Archean crust in the northern Wyoming province evidence from U-Pb ages of detrital zircons. Precambrian Res, 1998, 91: 295–307
31 Wilde S A, Valley J W, Peck W H, et al. Evidence from detrital zircons for the existence of continental crust and oceans on the Earth 4.4 Ga ago. Nature, 2001, 409: 175–178
32 Hartmann L A, Endo I, Suita M T F, et al. Provenance and age delimitation of Quadrilátero Ferrífero sandstones based on zircon U-Pb isotopes. J South Am Earth Sci, 2006, 20: 273–285
33 Gehrels G E, DeCelles P G, Ojha T P, et al. Geologic and U-Pb geochronologic evidence for early Paleozoic tectonism in the Dadeldhura thrust sheet, far-west Nepal Himalaya. J Asian Earth Sci, 2006, 28: 385–408
34 Kröner A, Hegner E, Lehmann B, et al. Palaeozoic arc magmatism in the Central Asian Orogenic Belt of Kazakhstan: SHRIMP zircon ages and whole-rock Nd isotopic systematics. J Asian Earth Sci, 2008, 32: 118–130
35 Wu F Y, Yang J H, Liu X M, et al. Nd isotopic constrains on crustal formation in the North China Craton. J Asian Earth Sci, 2005, 24: 523–545
36 Wilde S A, Valley J W, Kita N T, et al. SHRIMP U-Pb and CAMECA 1280 oxygen isotope results from ancient detrital zircons in the Caozhuang quartzite, eastern Hebei, North China Craton: Evidence for crustal reworking 3.8 Ga ago. Am J Sci, 2008, 308: 185–199
37 Nutman A P, Wan Y S, Du L L, et al. Multistage late Neoarchaean crustal evolution of the North China Craton, eastern Hebei. Precambrian Res, 2011, 189: 43–65
38 Wen C Q, Duo J, Fan X P, et al. Detrital Zircon of 4100Ma in Quartzite in Burang, Tibet (in Chinese). Acta Geol Sin, 2006, 80:

1249–1251
39 Duo J, Wen C Q, Guo J C, et al. 4.1 Ga old detrital zircon in western Tibet of China. Chin Sci Bull, 2007, 52: 23–26
40 Zhang S B, Zheng Y F, Wu Y B, et al. Zircon U-Pb age and Hf isotope evidence for 3.8 Ga crustal remnant and episodeic reworking of Archean crust in South China. Earth Planet Sci Lett, 2006, 252: 56–71
41 Wang H L, Chen L, Sun Y, et al. ~4.1 Ga xenocrystal zircon from Ordovician volcanic rocks in western part of North Qinling Orogen. Chin Sci Bull, 2007, 52: 3002–3010
42 Diwu C R, Sun Y, Dong Z C, et al. *In situ* U-Pb geochronolory of Hadean zircon xenocryst (4.1–3.9 Ga) from western of the Northern Qinling Orogen (in Chinese). Acta Petrol Sin, 2010, 26: 1171–1174
43 Zheng J P, Griffin W L, Tang H Y, et al. Archean basement similar to the North China and Yangtze continents may be existed beneath the Western Cathaysia (in Chinese). Geoll J Chin Univ, 2008, 14: 549–557
44 He S P, Li R S, Wang C, et al. Discovery of ~4.0 Ga detrital zircons in the Changdu Block, North Qiangtang, Tibetan Plateau. Chin Sci Bull, 2011, 56: 647–658
45 Chen B, Jahn B M. Genesis of post-collisional granitoids and basement nature of the Junggar Terrane, NW China: Nd-Sr isotope and trace element evidence. J Asian Earth Sci, 2004, 23: 691–703
46 Coleman R. Continental growth of Northwest China. Tectonics, 1989, 8: 621–625
47 Şengör A M C, Natal'in B A, Burtman V S. Evolution of the Altaid tectonic collage and Paleozoic crustal growth in Asia. Nature, 1993, 364: 299–307
48 Li J Y. Late Neoproterozoic and Paleozoic tectonic framework and evolutionof eastern Xinjiang, NW China (in Chinese). Geol Rev, 2004, 50: 304–322
49 Shu L S, Lu H F, Yin D H, et al. Late Paleozoic continental accretionary tectonics in Northern Xinjiang (in Chinese). Xinjiang Geol, 2001, 19: 59–63
50 Xiao W J, Han C M, Yuan C, et al. Middle Cambrian to Permian subduction-related accretionary orogenesis of North Xinjiang, NW China: Implications for the tectonic evolution of Central Asia. J Asian Earth Sci, 2008, 32: 102–117
51 Xiao W J, Windley B F, Yuan C, et al. Paleozoic multiple subduction-accretion processes of the southern Altaids. Am J Sci, 2009, 309: 221–270
52 Sun M, Long X P, Cai K D, et al. Early Paleozoic ridge subduction in the Chinese Altai: Insight from the abrupt change in zircon Hf isotopic compositions (in Chinese). Sci China Ser D-Earth Sci, 2009, 39: 935–948
53 Long X P, Yuan C, Sun M. Geochemistry and U-Pb detrital zircon dating of Paleozoic graywackes in East Junggar, NW China: Insights into subduction-accretion processes in the southern Central Asian Orogenic Belt. Gondwana Res, 2012, 21: 637–653
54 Wang H L, Xu X Y, He S P, et al. 1:1000000 Scale Geological Map of Tiansh and Its Adjacent Areas (in Chinese). Beijing: Geological Publishing House, 2007
55 He G Q, Li M S, Jia J D, et al. Significance of paleostruture and paleogeography of Ordovician-Silurian rock associations in Northern Xinjiang, China (in Chinese). Acta Sci Natur Univ Pekinensis , 2001, 37: 99–110
56 Li J Y. Main characteristics and emplacement processes of the East Junggar ophiolites, Xinjiang China (in Chinese). Acta Petrol Sin, 1995, 11: 73–84
57 Niu H C, Zhang H Y, Shan Q, et al. Geochemistry of the Nb-enriched basalt and its significance in Zaheba ophiolite mélange (in Chinese). Acta Petrol Sin, 2009, 25: 916–924
58 Niu H C, Zhang H Y, Shan Q, et al. Discovery of super-silicic and super-titanic garnels in garnet-pyroxenite in Zaheba and its significance, eastern Junggar, NW, China. Chin Sci Bull, 2008, 53: 2186–2191
59 Niu H C, Shan Q, Zhang H Y, et al. $^{40}Ar/^{39}Ar$ geochronology of the ultrahigh-pressure metamorphic quartz-magnesitite in Zhaheba, eastern Junggar, Xinjiang (in Chinese). Acta Petrol Sin, 2007, 23: 1627–1634
60 Niu H C, Shan Q, Zhang B, et al. Discovery of garnet amphibolite in Zaheba ophiolitic mélange, eastern Junggar, NW, China (in Chinese). Acta Petrol Sin, 2009, 25: 1484–1491
61 Jian P, Liu D Y, Zhang Q, et al. SHRIMP dating of ophiolite and leucocrutic rocks within ophiolite (in Chinese). Front Earth Sci, 2003, 10: 439–456
62 Zhang Y Y, Guo Z J. New constraints on formation ages of ophiolites in northern Junggar and comparative study on their connection (in Chinese). Acta Petrol Sin, 2010, 26: 422–430
63 Xiao W J, Windley B F, Yan Q R, et al. SHRIMP zircon age of the Aermantai ophiolite in the North Xinjiang area, China and its tectonic implications (in Chinese). Acta Geol Sci, 2006, 80: 32–37
64 The Second Regional Geological Survey Team of Xinjiang Bureau of Geology and Mineral Resources. 1:50000 ScaleJialepakeyizengde and Tasikake Regional Geological Survey Report (in Chinese). 1995
65 Regional Geological Measuring Team of Xinjiang Geological Bureau and Institute of Geology. 1:200000 Scale Aoshenkeshan Regional Geological Survey Report (in Chinese). 1966
66 Regional Geological Measuring Team of Xinjiang Geological Bureau and Institute of Geology. 1:200000 Scale Kamosite Regional Geological Survey Report (in Chinese). 1976
67 Regional Geological Measuring Team of Xinjiang Geological Bureau and Institute of Geology. 1:200000 Scale Qiakuertu Country Regional Geological Survey Report (in Chinese). 1966
68 Sláma J, Košler J, Daniel J, et al. Plesovice zircon—A new natural reference material for U-Pb and Hf isotopic microanalysis. Chem Geol, 2008, 249: 1–359
69 Li X H, Liu Y, Li Q L, et al. Precise determination of Phanerozoic zircon Pb/Pb ageby multicollector SIMS without external standardization. Geochem Geophys Geosyst, 2009, 10: Q04010
70 Andersen T. Correction of common Pb in U-Pb analyses that do not report ^{204}Pb. Chem Geol, 2002, 192: 59–79
71 Ludwig K R. Isoplot 3.0-A geochronological toolkit for Microsoft Excel. Berkeley Geochron Cent, Spec Publ, 2003, 4: 70
72 Yuan H L, Gao S, Dai M N, et al. Simultaneous determinations of U-Pb age, Hf isotopes and trace element compositions of zircon by excimer laser ablation quadrupole and multiple collector ICP-MS. Chem Geol, 2008, 247: 100–118
73 Bievre D P, Taylor P D. Table of the isotopic compositions of the elements. Int J Mass Spectrom Ion Process, 1993, 123: 149–166
74 Chu N C, Taylor R N, Chavagnac V, et al. Hf isotope ratio analysis using multi-collector inductively coupled plasma mass spectrometry: An evaluation of isobaric interference corrections. J Anal At Spectrom, 2002, 17: 1567–1574
75 Wu F Y, Yang Y H, Xie L W, et al. Hf isotopic compositions of the standard zircons and baddeleyites used in U-Pb geochronology. Chem Geol, 2006, 234: 105–126
76 Elhlou S, Belousova E, Griffin W L, et al. Trace element and isotopic composition of GJ red zircon standard by laser ablation. Geochim Cosmochim Acta, 2006, 70(Suppl): A158
77 Scherer E, Munker C, Mezger K. Calibration of the lutetium-hafnium clock. Science, 2001, 293: 683–687
78 Blichert-Toft J, Albarède F. The Lu-Hf isotope geochemistry of chondrites and the evolution of the mantle-crust system. Earth Planet Sci Lett, 1997, 148: 243–258
79 Vervoort J D, Blichert-Toft J. Evolution of the depleted mantle: Hf isotope evidence from juvenile rocks through time. Geochim Cosmochim Acta, 1999, 63: 533–556
80 Griffin W L, Pearson N J, Belousova E. The Hf isotope composition of cratonic mantle: LAM-MC-ICPMS analysis of zircon megacrysts in kimberlites. Geochim Cosmochim Acta, 2000, 64: 133–147
81 Amelin Y, Lee D C, Halliday A N. Nature of the Earth's earliest crust from hafnium isotopes in single detrital zircons. Nature, 1999, 399: 252–255
82 Harrison T M, Blichert-Toft J, Muller W, et al. Heterogeneous Hadean hafnium: Evidence of continental crust at 4.4 to 4.5 Ga. Science, 2005, 310: 1947–1950
83 Wu F Y, Zhao G C, Wilde S A, et al. Nd isotopic constraints on

crustal formation in the North China Craton. J Asian Earth Sci, 2005, 24: 523–545
84 Zhang Y, Liang G L, Qu X, et al. Evidence of U-Pb age and Hf isotope of zircons for Early Paleozoic magmatism in the Qiongheba arc, East Junggar (in Chinese). Acta Petrol Sin, 2010, 26: 2389–2398
85 Du S J, Qu X, Deng G, et al. Chronology and tectonic setting of the intrusive bodies and associated porphyry copper deposit in Hersai area, East Junggar (in Chinese). Acta Petrol Sin, 2010, 26: 2981–2996
86 Guo H C, Zhong L, Li L Q, et al. Zircon SHRIMP U-Pb dating of quartz diorite in the Koumenzi area, Karlik Mountains, East Tianshan, Xinjiang, China, and its geological significance (in Chinese). Geol Bull Chin, 2006, 25: 928–931
87 Cao F Y, Tu Q J, Zhang X M, et al. Preliminary determination of the Early Paleozoic magmatic arc in the Karlik Mountains, East Tianshan, and Xinjiang, China: Evidence from zircon SHRIMP U-Pb dating of granite bodies in the Tashuihe (in Chinese). Geol Bull Chin, 2006, 25: 923–927
88 Li J Y, Wang K Z, Sun G H, et al. Paleozoic active margin slices in the southern Turfan-Hami basin: geological records of subduction the Paleo-Asian Ocean plate in central Asian regions (in Chinese). Acta Petrol Sin, 2006, 22: 1087–1102
89 Sun M, Yuan C, Xiao W J, et al. Zircon U-Pb and Hf isotopic study of gneissic rocks from the Chinese Altai: Progressive accretionary history in the early to middle Paleozoic. Chem Geol, 2008, 247: 352–383
90 Wang T, Hong D W, Jahn B, et al. Timing, petrogenesis and setting of Paleozoic synorogenic intrusions from the Altai Mountains, Northwest China: Implications for the tectonic evolution of an accretionary orogen. J Geol, 2006, 114: 735–751
91 Ceng Q S, Chen G H, Wang H, et al. Geochemical characteristic, SHRIMP zircon U-Pb and tectonic implication for granitoids in Chonghuer basin, Altai, Xinjiang (in Chinese). Acta Petrol Sin, 2007, 23: 1921–1932
92 Liu F, Li Y H, Mao J W, et al. SHRIMP U-Pb ages of the Abagong granites in the Altay Orogen and their geological implications (in Chinese). Acta Geosci Sin, 2007, 23: 1921–1932
93 Wong K, Sun M, Zhao G C, et al. Geochemical and geochronological studies of the Alegedayi ophiolitic complex and its implication for the evolution of the Chinese Altai. Gondwana Res, 2010, 18: 438–454
94 Cai F M, Dong L H, Yang F Q, et al. Age, geochemistry and petrogenesis of Tiemerte granites in the Kelang basin at the southern margin of Altai, Xinjiang (in Chinese). Acta Petrol Sin, 2007, 23: 1921–1932
95 Wang T, Tong Y, Li S, et al. Spatial and temporal variations of granitoids in the Altay Orogen and their implications for tectonic setting and crustal growth: perspectives from Chinese Altay (in Chinese). Acta Petrol Et Miner, 2010, 29: 595–618
96 Long X P, Yuan C, Sun M. Detrital zircon ages and Hf isotopes of the early Paleozoic flysch sequence in the Chinese Altai, NW China: New constrains on depositional age, provenance and tectonic evolution. Tectonophys, 2010, 480: 213–231
97 Cai K D, Sun M, Yuan C, et al. Prolonged magmatism, juvenile nature and tectonic evolution of the Chinese Altai, NW China: Evidence from zircon U-Pb and Hf isotopic study of Paleozoic granitoids. J Asian Earth Sci, 2011, 42: 949–968
98 Wang Y J, Yuan C, Long X P, et al. Geochemistry, zircon U-Pb ages and Hf isotopes of the Paleozoic volcanic rocks in the northwestern Chinese Altai: Petrogenesis and tectonic implications. J Asian Earth Sci, 2011, 42: 969–985
99 Wang Y J, Liu H J, Zhou J P, et al. LA-ICP-MS U-Pb dating of detrital zircons from the marine volcanic-sedimentary rocks in the northern Kamste, Eastern Junggar and its geological significance (in Chinese). Geoscience, 2011, 25: 1047–1058
100 Li Y P, Li J Y, Sun G H, et al. Basement of Junggar basin: Evidence from detrital zircons in sandstone of previous Devonian Kalamaili formation (in Chinese). Acta Petrol Sin, 2007, 23: 1577–1590
101 Huang G, Niu G Z, Wang X L, et al. Formation and emplacement age of Karamaili ophiolite: LA-ICP-MS zircon U-Pb age evidence from the diabase and tuff in eastern Junggar, Xinjiang (in Chinese). Geol Bull Chin, 2012, 31: 1267–1278
102 Li J Y, He G Q, Xu X, et al. Crustal tectonic framework of Northern Xinjiang and adjacent regions and its formation (in Chinese). Acta Geol Sin, 2006, 80: 148–167
103 Jiang Y J, Yang B Z, Wang Y Y, et al. Structural feature and evolution in northeast part of Junggar basin (in Chinese). Acta Geol Sin, 2002, 76: 462–468
104 Li H O, Jiang M, Wang Y J, et al. Image of crust and upper mantle structure along the array from Fuyun to Kuerle by P–to–S converted waves (in Chinese). Acta Geol Sin, 2006, 80: 135–141
105 Wang Y J, Qian R Y, Jiang M, et al. Image of crust and upper mantle velocity structure along the array from Fuyun to Kuerle by seismic tomography (in Chinese). Acta Geol Sin, 2006, 80: 142–147
106 Su Y Z. On the geological and geographical distribution of Tuvaella with reference to its habitat (in Chinese). Acta Palaeont Sin, 1981, 20: 567–576
107 Zhang Z X, Rong J Y, Di Q L. Silurian Tuvaella gigantean faunule of the Barkol area, Northeastern Xinjiang (in Chinese). Acta Palaeont Sin, 1983, 22: 278–294